

# 1

## Transport of Dirac Surface States

---

D. Carpentier

### 1.1 Introduction

#### 1.1.1 Purpose of the lectures

The occurrence of robust states at their surface is the most salient feature of three dimensional topological insulators [29, 47]. Indeed, it is their existence in ARPES experiments which is used as a signature of the topological property of the bulk bands. These surface states turn out to be described by a relativistic two dimensional Dirac equation at low energy. In these short lectures, we focus on the transport properties of these Dirac surface states. While transport may not be the ideal probe of the existence of Dirac-like electronic excitations, it remains a tool of choice in condensed matter. In the following, we survey some of the transport properties of Dirac excitations and the techniques appropriate to their studies. For the sake of pedagogy, we will focus on simplest transport properties, neglecting in particular transport in hybrid structures with superconductors which would deserve their own lectures.

Naturally, there is a strong overlap between the study of transport properties of graphene and surface states of topological insulators. Indeed the low energy electronic excitations of graphene are also described as two dimensional Dirac particles. The recent discovery of graphene has led to a large amount of work on the associated transport properties : there already exist textbooks and extensive reviews on the subject including [10, 19, 20, 35, 24] and [14, 65] on related matter. In the context of topological insulator surface states, the review [12] focuses on the quantum coherent transport properties. In these lectures, we start by a survey of classical transport properties of Dirac fermions at high carrier concentration and the inherent anisotropic scattering using Boltzmann equation. The minimum conductivity of evanescent Dirac states in a short junction is described within Landauer formalism. Then the quantum coherent regime is approached within the diagrammatic perturbation theory and Kubo formula, in the spirit of [4]. This technique also allows to recover the results on classical transport at zero and high chemical potentials.

## 2 Transport of Dirac Surface States

### 1.1.2 Dirac Surface States of Topological Insulators

*Generic Hamiltonian.* We will neglect the consequence of the possible presence of conducting bulk states in the insulating gap. While in current experiments these states are present we prefer to focus on the simpler ideal situation for pedagogical reasons. A more realistic treatment should include the coupling between the surface and these bulk states. While the surface of topological insulators is generically characterized by an odd number of Dirac species [29, 47] we consider in the following the simplest situation described by a single Dirac cone. For energies lying in the bulk gap, electronic states are described as eigenstates of the low energy Bloch Hamiltonian

$$H(\vec{k}) = \hbar v_F \vec{\sigma} \cdot \vec{k}, \quad (1.1)$$

where  $\vec{k}$  is the two dimensional momentum along the surface and  $\vec{\sigma}$  represents two Pauli matrices for an effective spin  $\frac{1}{2}$ . The momentum-spin locking for eigenstates of the Hamiltonian (1.1) is reminiscent of the bulk spin-orbit coupling at the origin of the bulk band inversion. The hamiltonian (1.1) is invariant by a so-called symplectic time reversal symmetry  $T$  which satisfies  $T^2 = -\mathbf{I}$  [66, 21, 71] :  $TH(\vec{k})T^{-1} = H(-\vec{k})$  with  $T = i\sigma_y \mathcal{C}$ ,  $\mathcal{C}$  denoting the complex conjugation operator acting on the right. We choose to write the eigenstates of (1.1) as

$$|u(\vec{k} = k e^{i\theta})\rangle = \frac{1}{\sqrt{2}} \begin{pmatrix} 1 \\ \pm e^{i\theta} \end{pmatrix} \text{ with } \epsilon(\vec{k}) = \pm v_F \hbar k. \quad (1.2)$$

Note that the hamiltonian (1.1) is also relevant to discuss the transport at the surface of weak topological insulators or crystalline topological insulators characterized by an even number of Dirac cone but with a symplectic time reversal symmetry [48], quantum wells close to a topological transition in which case a small mass term  $m\sigma_z$  should be added [60], and other realizations (see [63] for a recent discussion of Dirac matter).

*Hexagonal warping.* For energies far away from the Dirac point, the linearized Hamiltonian (1.1) has to be complemented by higher order terms, leading to a warping of the Fermi-surface. In the case of the surface states of  $\text{Bi}_2\text{Te}_3$ , this warping corresponds to an hexagonal deformation of the Fermi surface, and is due to an additional term in the Hamiltonian for surface states

$$H_w = \frac{\lambda}{2} \sigma_z (k_+^3 + k_-^3), \quad (1.3)$$

with  $k_{\pm} = k_x \pm ik_y$ . The resulting hexagonal symmetry of the Fermi surface originates from the combination of a trigonal discrete  $C_3$  lattice symmetry with time reversal symmetry [28, 39]. The corresponding dispersion relation  $\epsilon^2(\vec{k} = k e^{i\theta}) = \hbar^2 v_F^2 k^2 + \lambda^2 k^6 \cos^2(3\theta)$  leads to the snowflake shape of constant energy surfaces [3]. Defining  $\epsilon_F = \hbar v_F k_F$  and  $k = k_F \tilde{k}(\theta)$ , the shape of the Fermi surface at energy  $\epsilon_F$  is conveniently parametrized by the dimensionless parameter  $b = \lambda E_F^2 / (2\hbar^3 v_F^3)$  as

$$1 = \tilde{k}^2(\theta) + 4b^2 \tilde{k}^6(\theta) \cos^2(3\theta). \quad (1.4)$$

While this parameter takes reasonable small values  $0.04 < b < 0.09$  for energies  $0.05\text{eV} < \epsilon_F < 0.15\text{eV}$  for the  $\text{Bi}_2\text{Se}_3$  compound, it ranges from  $b = 0.13$  for  $\epsilon_F = 0.13$

eV to  $b = 0.66$  for  $\epsilon_F = 0.295$  eV in  $\text{Bi}_2\text{Te}_3$  and leads to sizable consequences on transport at high chemical potential [3].

*Disorder.* Transport amounts to describe scattering of electronic excitations, in particular on impurities. In the following, we adopt a statistical description of these impurities : we describe them by a continuous field corresponding to an additional term  $V(\hat{r}) \mathbf{1}$  in the Hamiltonian. This field is random, and its realizations are chosen according to a characteristic distribution  $P[V]$ . For simplicity, we adopt the simplest convention corresponding to a gaussian distribution, with vanishing average  $\langle V(\hat{r}) \rangle_V = 0$  and variance

$$\langle V(\hat{r})V(\hat{r}') \rangle_V = \gamma_V(\hat{r} - \hat{r}') \quad (1.5)$$

where  $\langle \rangle_V$  corresponds to an average over disorder configurations and the correlation  $\gamma_V(\hat{r})$  is exponentially decaying over a short distance  $\xi$ . We will often approximate it by a  $\delta$  function in the continuum limit.

This gaussian distributed potential can be recovered as the continuum limit of the Edwards model of localized impurities [4]. Indexing independent impurities by  $j$  the corresponding random potential is written as  $\hat{V}(\hat{r}) = \sum_j \hat{v}(\hat{r} - \vec{R}_j)$ , where  $\hat{v}(\vec{r}) = v(\vec{r}) \mathbf{I}$  couples only to the density of Dirac fermions. The averaged matrix elements of this potential between Dirac eigenstates are

$$\langle |\langle \vec{k} | V | \vec{k}' \rangle|^2 \rangle_V = n_i |v(\vec{k}, \vec{k}')|^2 \left| \langle u(\vec{k}') | u(\vec{k}) \rangle \right|^2 \equiv \gamma_V(\vec{k}, \vec{k}') \left| \langle u(\vec{k}') | u(\vec{k}) \rangle \right|^2, \quad (1.6)$$

where  $n_i$  is the impurity concentration. In the limit  $n_i \rightarrow \infty$ ,  $v(\vec{k}, \vec{k}') \rightarrow 0$  while keeping  $\gamma_V(\vec{k}, \vec{k}') = n_i |v(\vec{k}, \vec{k}')|^2$  constant we recover a gaussian continuous random field. A more realistic treatment of the disorder encountered at the surface of topological insulators, along the lines of [38], goes beyond the scope of these lectures.

### 1.1.3 Graphene

*Low Energy Bloch Hamiltonian.* Graphene consists in a hexagonal lattice of Carbon atoms whose electronic properties can be described by considering a single  $p_z$  atomic orbital per lattice site. The electronic Bloch wave function are naturally decomposed on the two sub-lattices of the hexagonal lattice according to  $\psi(\vec{k}, \vec{x}) = e^{i\vec{k}\cdot\vec{x}} \left( u_A(\vec{k}, \vec{x}) + u_B(\vec{k}, \vec{x}) \right)$ . The corresponding Bloch Hamiltonian acting on the functions  $u_{A/B}(\vec{k}, \vec{x})$  is written as

$$H(\vec{k}) = \begin{pmatrix} g(\vec{k}) & f(\vec{k}) \\ \bar{f}(\vec{k}) & g(\vec{k}) \end{pmatrix}. \quad (1.7)$$

At low energy, only nearest neighbor hopping integrals can be kept, imposing vanishing amplitudes diagonal in sub-lattice  $g(\vec{k}) = 0$ , and hopping between different sub lattices  $f(\vec{k})$  which vanishes at the two Dirac points  $\vec{K}$  and  $\vec{K}' = -\vec{K}$ . The existence of two cones, associated with states of opposites chiralities at a given energy, is a consequence of the Nielsen-Ninomiya theorem [44] which states the impossibility to realize a lattice

#### 4 Transport of Dirac Surface States

model with realistic couplings but a net chirality among its excitations [33]. Hence for small energies eigenstates are labeled by a quasi-momentum close to either  $\vec{K}$  or  $\vec{K}'$  : it is thus convenient to introduce a 'valley index' and write an effective Hamiltonian in this extended basis. By using  $f(\pm\vec{K} + \vec{q}) = \hbar v_F(\pm q_x - i q_y)$  we write the corresponding Hamiltonian as

$$H(\vec{q}) = \begin{pmatrix} H(\vec{K} + \vec{q}) & 0 \\ 0 & H(\vec{K}' + \vec{q}) \end{pmatrix} = \begin{pmatrix} \hbar v_F \vec{\sigma} \cdot \vec{q} & 0 \\ 0 & \hbar v_F \vec{\sigma} \cdot \vec{q} \end{pmatrix} \quad (1.8)$$

where  $H(\vec{q})$  acts on vectors of states ( $|u_{\vec{K},A}(\vec{k})\rangle, |u_{\vec{K},B}(\vec{k})\rangle, -|u_{\vec{K}',B}(\vec{k})\rangle, |u_{\vec{K}',A}(\vec{k})\rangle$ ) with the definition  $|u_{A/B}(\pm\vec{K} + \vec{q})\rangle = |u_{\vec{K}/\vec{K}',A/B}(\vec{q})\rangle$ .

*Time-Reversal Symmetry.* The Hamiltonian (1.7) describes spinless fermions on the hexagonal lattice : the spectrum for the electrons is spin degenerate and described neglecting spin degree of freedom. Hence this Hamiltonian is invariant by time-reversal symmetry for spinless electrons : if  $\psi(\vec{k}, \vec{x})$  is an eigenstate of energy  $\epsilon_{\vec{k}}$  then  $\bar{\psi}(\vec{k}, \vec{x})$  is also an eigenstate of same energy, where we use the notation  $\bar{\psi}(\vec{k}, \vec{x}) = \mathcal{C}\psi(\vec{k}, \vec{x})$  for the complex conjugate of  $\psi(\vec{k}, \vec{x})$ . This symmetry manifests itself as  $\bar{H}(-\vec{k}) = H(\vec{k})$  on the Bloch Hamiltonian (1.7). Expressed in the valley / sub-lattice Hilbert space, it is written as

$$TH(\vec{q})T^{-1} = H(-\vec{q}) \quad ; \quad T = (i\tau_y \otimes i\sigma_y) \mathcal{C}. \quad (1.9)$$

This anti-unitary time reversal operator satisfies  $T^2 = \mathbf{I}$ , as expected for spinless particles. Due to the emergence of the pseudo-spin  $\frac{1}{2}$  in sub-lattice space, the low energy Hamiltonian  $H(\vec{q})$  possesses a second time-reversal symmetry acting in each valley on spin  $\frac{1}{2}$  fermions [14]:

$$\tilde{T}H(\vec{q})\tilde{T}^{-1} = H(-\vec{q}) \quad ; \quad \tilde{T} = (\mathbf{I} \otimes i\sigma_y) \mathcal{C}, \quad (1.10)$$

which is a symplectic symmetry :  $\tilde{T}^2 = -\mathbf{I}$ . Two time reversal symmetries, which are defined as anti-unitary operators commuting with the Hamiltonian, necessarily differ by a unitary operator which commutes with the Hamiltonian : a standard symmetry [50]. Here, this symmetry emerges in the low energy regime and consists in the exchange of valleys (without reversal of momenta  $\vec{q}$ ) :  $U = i\tau_y \otimes \mathbf{I}$ . The presence of these two time-reversal symmetries, an orthogonal and a symplectic one, leads to a possible cross-over between universality classes of phase-coherent weak localization physics : this cross-over is controlled by the correlation of the disorder, and more precisely whether the  $U$  symmetry is statistically preserved, *i.e.* whether disorder correlation is diagonal in valley index [59] (see also [5, 42] for more realistic and complex descriptions at low energy). In the present lectures, we focus on transport properties of a single Dirac cone corresponding to the situation where the total Hamiltonian including disorder is valley-diagonal, *i.e.* is invariant under the symmetry  $U$ .

##### 1.1.4 Overview of the transport properties

The typical behavior of the electrical conductivity of Dirac fermions is represented in figure 1.1. A remarkable feature is the existence of a non vanishing conductivity at the

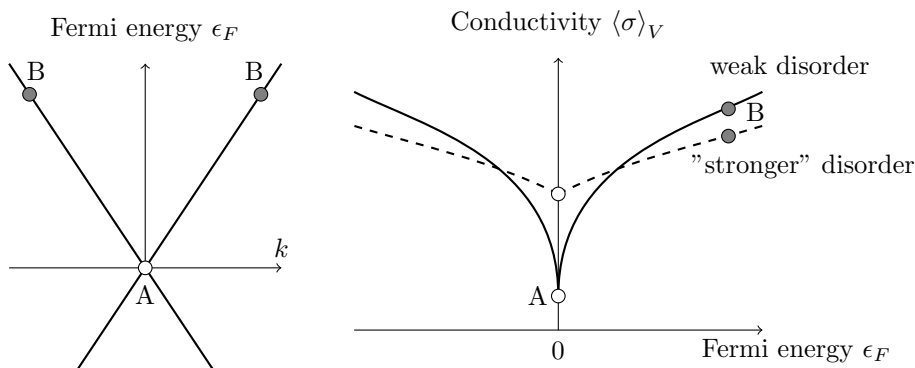


**Fig. 1.1** Schematic behavior of the conductivity as a function of the Fermi energy (right) for a Dirac dispersion relation (left). A characteristic feature is the existence of a finite conductivity at the Dirac point (point A), which increases with the disorder amplitude. At higher energies, a more common diffusive metallic behavior is recovered (point B), with intrinsically anisotropic scattering properties.

Dirac point even in the absence of disorder [25,26,69,54,46,62,34]. We expect the transport in this limit to be unconventional and quantum in nature as the Fermi wavelength becomes increasingly large close to the Dirac point. Indeed, this conductivity at the Dirac point was shown to correspond to a "pseudo-diffusive" regime, with a statistics of transmission coefficients characteristic of diffusive transport in conventional metals [62]. We will discuss this minimal conductivity in the clean limit in a tunnel barrier geometry where it is related with the transport through evanescent Dirac states [62], and its possible relation with the so-called Zitterbewegung of Dirac fermions [34]. When disorder is increased, both the density of states at the Dirac point and the associated conductivity increase. This increase can be described using a self-consistent Born approximation [54], or alternatively a self-consistent Boltzmann approach which can be extended to the regime at high Fermi energies [2]. In this last approach, the density of states is renormalized by the fluctuations of disorder or chemical potential, which become dominant at very low Fermi energy:  $\tilde{\epsilon}_F = (\langle(\epsilon + V)^2\rangle_V)^{\frac{1}{2}}$ . The quantum regime of weak disorder is difficult to accurately describe within this Boltzmann approach [1]. The behavior at stronger disorder in this quantum low energy regime is a manifestation of the absence of Anderson localization for a model of a single Dirac cone of fermions [45,13,51]. These Dirac fermions are the signature of the bulk topological property of valence bands: they cannot be gapped out, in particular by disorder (provided the bulk gap does not close) [53]. This property was later used to obtain a classification of topological phases, identifying those that allowed surface states robust towards Anderson localization [50].

At higher Fermi energies (point B in Figure 1.1), we recover a standard situation where the Fermi-wavelength is much smaller than characteristic lengths for transport, including the mean free path: a semi-classical approach *via* the Boltzmann equation is possible. As we will see, in this regime the manifestation of the Dirac nature of

## 6 Transport of Dirac Surface States

the electrons lies in the anisotropy of scattering, even in the presence of "isotropic impurities". Naturally this property requires the use of a transport time, different from the elastic scattering time, to define the diffusion constant. For small samples in which transport can remain phase coherent over sizable distances, quantum corrections to this diffusive transport have to be taken into account. The standard description of this quantum regime was extended to the case of Dirac diffusion in the context of graphene [5,42,36,43,6]. In this context, the result depends on the type of disorder and its symmetry with respect to valley indices : we obtain a standard weak-localization physics (orthogonal class), or weak anti-localization (symplectic class). The situation of Dirac surface states of topological insulators is simpler as no cross-over is allowed without magnetic disorder. We will describe this regime, following the diagrammatic approach in the spirit of [4]. We will not discuss the Altshuler - Aronov effect. The interested reader can turn to [52] for an alternative and interesting description of the semi-classical regime for Dirac fermions as a propagation along classical trajectories.

### 1.2 Minimal conductivity close to the Dirac point

#### 1.2.1 Zitterbewegung

The transport in the limit  $\epsilon_F \rightarrow 0$  has been related to the peculiar nature of Dirac fermions [62,34]. In particular, the occurrence of a finite conductivity in the clean limit was discussed in relation with the Zitterbewegung *i.e.* an intrinsic agitation of Dirac fermions [34]. Indeed, the current operator  $\vec{j} = ev_F \vec{\sigma}$  associated with Hamiltonian (1.1) does not commute with it. Hence  $\langle \vec{j} \rangle$  is not a constant of motion for eigenstates of the Hamiltonian, which signals the existence of a "trembling motion" or Zitterbewegung, around the center of motion [64]. This Zitterbewegung was claimed to play the role of an intrinsic disorder manifesting itself in a finite conductivity at  $\epsilon_F = 0$  [34,35]. Of particular interest is the geometry of a large "tunnel" junction of Dirac material at the Dirac point. Let us express the current operator in the eigenstates basis (1.2) of the Hamiltonian (1.1) with  $\vec{k} = ke^{i\theta}$  :

$$j_x = ev_F \begin{pmatrix} \cos \theta & i \sin \theta e^{-i\theta} \\ -i \sin \theta e^{i\theta} & -\cos \theta \end{pmatrix} ; \quad j_y = ev_F \begin{pmatrix} \sin \theta & -i \cos \theta e^{-i\theta} \\ i \cos \theta e^{i\theta} & -\sin \theta \end{pmatrix}. \quad (1.11)$$

In this basis, the non-commutativity of  $\vec{j}$  with the Hamiltonian originates from the off-diagonal terms describing transitions between the  $\pm v_F \hbar k$  eigenstates. It is natural to expect this Zitterbewegung to manifest itself strongly close to the Dirac point and in the presence of broadening of the eigenstates originating from either disorder or confinement. This is indeed what occurs.

#### 1.2.2 Clean Large Tunnel Junction

Following [62], we consider a wide barrier at the surface of a topological insulator, such that the length of the barrier  $L$  is much smaller than its circumference  $W$  around the sample, as shown on figure 1.2. The confinement of the tunnel junction is described by the potential  $eV(x) \mathbf{1}$  added to the Hamiltonian (1.1) with  $V(x) = 0$  exactly at the Dirac point for  $0 < x < L_x$  and  $V(x) = V_\infty$  outside of the barrier ( $x < 0$  and  $x > L$ ). The periodic boundary condition in the  $y$  direction around the sample implies

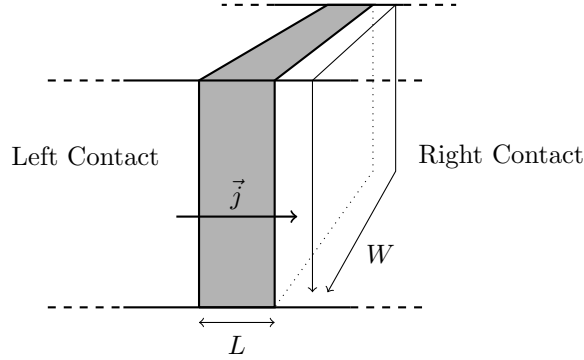


**Fig. 1.2** Schematic representation of a tunnel junction at the surface of a topological insulator. In the ideal situation, for a chemical potential inside the bulk gap, only the Dirac surface states transport the current between the contacts.

the quantization of momentum along  $y$ :  $k_n = n2\pi/W$  with  $-W/2 \leq n \leq W/2$ . The conductance of the junction can then be deduced from the Landauer formula [32]

$$G = \frac{W}{L} \sigma = \frac{e^2}{h} \sum_n T_n, \quad (1.12)$$

where the  $T_n$  denote the transmission coefficients of the current carried by the different modes of the junction. At  $\epsilon = 0$  only evanescent states carry current in the junction. They are described by the eigenfunctions

$$\psi(x, y) = \frac{1}{\sqrt{2}} \begin{pmatrix} ae^{k_n x} \\ be^{-k_n x} \end{pmatrix} e^{ik_n y}. \quad (1.13)$$

We recover here a crucial property of the Dirac Hamiltonian (1.1) : at each boundary  $x = 0$  or  $x = L$ , these evanescent states are entirely polarized in either the  $\uparrow$  or  $\downarrow$  state (corresponding to localization in a single sub lattice in the case of graphene). This is a consequence of the chiral symmetry of the Dirac Hamiltonian [30]: the operator  $C = \sigma_z$  anticommutes with the Hamiltonian (1.1). Hence  $C$  relates eigenstates at  $+\epsilon(\vec{k})$  to eigenstates at  $-\epsilon(\vec{k})$ . However at  $\epsilon(\vec{k}) = 0$  this chirality symmetry implies that all eigenstates of the Hamiltonian are also eigenstates of  $C$ . The conductance at  $\epsilon = 0$  directly probes transport property of these chirality eigenstates, although in their evanescent form.

We can now solve the standard diffusion problem through the potential well and find the transmission coefficients

$$T_n(\vec{k} = ke^{i\theta}) = \frac{\cos^2 \theta}{\cosh^2(k_n L) - \sin^2 \theta} \simeq \frac{1}{\cosh^2 k_n L} \text{ for large } V_\infty \text{ i.e. } k_x \gg k_n. \quad (1.14)$$

In the limit of a wide and narrow junction  $W \gg L$ , the ensemble of transmission coefficients  $T_n$  samples accurately the underlying distribution function  $\rho(T)$  and we find a dimensionless conductance

## 8 Transport of Dirac Surface States

$$g = \frac{G}{e^2/h} = \sum_{n=-\infty}^{+\infty} T_n \simeq \frac{W}{2\pi L} \int_{-\pi L}^{+\pi L} \frac{1}{\cosh x} dx = \frac{W}{\pi L}. \quad (1.15)$$

This result corresponds to a minimal conductivity  $\sigma_{\min} = e^2/(\pi h)$ . Quite remarkably the transmission coefficients are distributed according to the law [62]

$$\rho(T) = \frac{g}{2T\sqrt{1-T}}, \quad (1.16)$$

characteristic of the conventional orthogonal diffusive metallic regime. Accordingly, the tunnel transport through a wide Dirac junction has been denoted a pseudo-diffusive regime. The occurrence of the diffusive distribution function of transmissions explains the identification between this tunnel conductivity and the diffusive conductivity of long wide conductor in the presence of weak disorder presented in the following section.

### 1.2.3 Minimal conductivity from linear response theory

The above minimum conductance at the Dirac point in the clean limit can be recovered in the case of a large sample of size  $L = W$  by using the Kubo formula. We follow the approach of [49] (see also the earlier work [40]) and consider the Kubo formula for the conductivity calculated within linear response theory :

$$\sigma_{ij}(\omega, \beta, \tau) = \frac{\hbar}{4\pi L^2} \int d\epsilon \frac{f_\beta(\epsilon + \hbar\omega) - f_\beta(\epsilon)}{\hbar\omega} \text{Tr} \left( \text{Im} \hat{\mathcal{G}}^A(\epsilon, \tau) \hat{j}_i \text{Im} \hat{\mathcal{G}}^A(\epsilon + \hbar\omega, \tau) \hat{j}_j \right), \quad (1.17)$$

where  $f_\beta(\epsilon)$  is the Fermi-Dirac distribution function, the current density operator reads  $\vec{j} = ev_F \vec{\sigma}$  and the trace runs over the quantum numbers (spin and momentum) of electronic states. In this expression  $\text{Im} \hat{\mathcal{G}}^A(\epsilon, \tau) = \hat{\mathcal{G}}^A(\epsilon, \tau) - \hat{\mathcal{G}}^R(\epsilon, \tau)$  where  $\hat{\mathcal{G}}^{R,A}$  correspond to the retarded and advanced Green functions for the hamiltonian (1.1), with or without disorder potential  $V$  :

$$\hat{\mathcal{G}}^{R/A}(\vec{k}, \epsilon, \tau_\phi) = \left[ \left( \epsilon \pm i \frac{\hbar}{2\tau_\phi} \right) \mathbf{I} - H(\vec{k}) - V \right]^{-1}. \quad (1.18)$$

Here  $\tau$  stands either to an elastic mean free time  $\tau_e$  in the disorder case, or a phenomenological phase coherent time  $\tau_\phi(T)$  for the Bloch states accounting for the inelastic interactions of the electron with the phonons, other electrons, or magnetic Kondo impurities [32]. In the presence of disorder, we approximate the average of the conductivity over disorder  $\langle \sigma \rangle_V$  by replacing the Green's function in eq. (1.17) by their average over disorder (see section 1.3.2 for a discussion of this point and refinements). This simply amounts to replace the phase coherence time  $\tau_\phi$  by the shorter elastic mean free time  $\tau_e$  (see eq. (1.46),(1.48)). The (averaged) Green's functions for the Dirac fermions are written as

$$\mathcal{G}^{R/A}(\vec{k}, \epsilon, \tau) = \frac{(\epsilon \pm i\hbar/2\tau)\mathbf{I} + \hbar v_F \vec{k} \cdot \vec{\sigma}}{(\epsilon \pm i\hbar/2\tau)^2 - \epsilon^2(\vec{k})}. \quad (1.19)$$

The trace over spin space in the expression (1.17) can now be performed. The remaining order of limits is crucial : we keep  $\tau$  finite and using

$$\lim_{\beta \rightarrow \infty} \lim_{\omega \rightarrow 0} \frac{f_{\beta}(\epsilon + \hbar\omega) - f_{\beta}(\epsilon)}{\hbar\omega} = -\delta(\epsilon),$$

we obtain the minimal conductivity (using  $\eta^{-1} = 2\tau$ ) :

$$\lim_{\beta \rightarrow \infty} \lim_{\omega \rightarrow 0} \sigma_{ij}(\omega, \beta, \tau) = \frac{2}{\hbar} \left( \frac{ev_F}{2\pi} \right)^2 \int_0^{\infty} dx \frac{\eta^2}{(\eta^2 + v_F^2 x)^2} = \frac{e^2}{\pi\hbar}, \quad (1.20)$$

which is precisely the result found for the wide and narrow junction using Landauer formula. Note that a finite  $\eta$  or  $\tau$  was crucial in deriving this result : its presence is related in the clean case to either a dephasing time in the large sample geometry, or a lifetime in the sample due to the presence of the absorbing boundaries for a narrow strip considered in the previous section. The independence of the result (1.20) on  $\tau$  and thus on a weak disorder breaks down as the disorder strength is increased, as shown in numerical studies [1], and in agreement with contribution of the quantum correction (weak anti-localization) described in section 1.4.

### 1.3 Classical conductivity at high Fermi energy

At higher Fermi energies, represented schematically as the region of point  $B$  in figure 1.1, we recover a conventional situation of a metal with a Fermi wavelength  $2\pi/k_F$  much smaller than length scales characteristics of transport (mean free path  $l_e$  or the size of the sample  $L$ ). This regime is conveniently described using a semi-classical description. First we will identify the signature of the Dirac nature of excitations within the Boltzmann equation approach, before resorting to the Kubo approach previously introduced.

#### 1.3.1 Boltzmann Equation

Classical phase space is spanned by variables  $\vec{r}_c, \vec{p}_c$  : a statistical description of an ensemble of particles amounts to define a density of states  $f(\vec{r}_c, \vec{p}_c, t)$  at time  $t$ . The Boltzmann equation states that the evolution of this density of states is the sum of three terms

$$\frac{\partial f}{\partial t} = -\frac{d\vec{r}_c}{dt} \cdot \vec{\nabla}_{\vec{r}_c} f - \frac{d\vec{p}_c}{dt} \cdot \vec{\nabla}_{\vec{p}_c} f + I[f], \quad (1.21)$$

where  $I[f]$  is a collision integral defined below in eq. (1.31), which describes the evolution of the density  $f$  due to scattering. To proceed in this semi-classical description of electrons in crystals, we need equations of motions for  $d\vec{r}_c/dt$  and  $d\vec{p}_c/dt$ . It has been recently understood that these equations not only depend on the band structures  $\epsilon(\vec{k})$  but also on geometrical properties of the field of eigenvectors associated with these bands [67]. Although these geometrical characteristics do not enter the simplest transport properties addressed in these lectures, it is interesting to introduce them for extensions to e.g. the magneto-transport. Let us sketch briefly the derivation of these semi-classical equations of motion [67, 41].

## 10 Transport of Dirac Surface States

*Semi-classical equations of motion.* We want to describe the time evolution of a semi-classical wave packet restricted to a single band indexed by  $n$  (or more generally a subset of bands). This amounts to consider a wave packet

$$|\psi_{\vec{r}_c, \vec{k}_c}^{(n)}\rangle = \int \frac{d^2\vec{k}}{(2\pi)^2} \chi(\vec{k} - \vec{k}_c) e^{-i(\vec{k} + \frac{e}{\hbar c} \vec{A}(\vec{r}_c)) \cdot \vec{r}_c} |\psi(\vec{k}, n)\rangle, \quad (1.22)$$

where  $\langle \vec{r} | \psi(\vec{k}, n) \rangle = e^{i\vec{k} \cdot \vec{r}} \langle \vec{r} | u(\vec{k}, n) \rangle$  are eigenstates associated with the band  $n$ , and the vector potential  $\vec{A}$  originates from the possible presence of a magnetic field. Imposing the localisation of the wave packet around  $\vec{r}_c$ , *i.e.*

$$\langle \psi_{\vec{r}_c, \vec{k}_c}^{(n)} | \hat{r} | \psi_{\vec{r}_c, \vec{k}_c}^{(n)} \rangle = \vec{r}_c, \quad (1.23)$$

imposes that the phase of  $\chi(\vec{k} - \vec{k}_c)$  is related to the Berry connexion in band  $n$  :

$$\chi(\vec{k} - \vec{k}_c) = |\chi(\vec{k} - \vec{k}_c)| e^{i(\vec{k} - \vec{k}_c) \cdot \vec{A}^{(n)}(\vec{k}_c)}. \quad (1.24)$$

In this expression,  $\vec{A}^{(n)}(\vec{k}_c)$  is not a connexion defined on the field of electronic states  $|\psi(\vec{k}, n)\rangle$ , but on the states  $|u(\vec{k})\rangle = \exp(-i\vec{k} \cdot \hat{r}) |\psi(\vec{k})\rangle$  invariant by translations on the lattice. These states are eigenstates of the  $\vec{k}$ -dependent Bloch Hamiltonian  $H(\vec{k}) = \exp(i\vec{k} \cdot \hat{r}) H \exp(-i\vec{k} \cdot \hat{r})$ . Following M. Berry [17] we can define a connexion  $\vec{A}^{(n)}(\vec{k}_c)$  associated to the parallel transport within the space of eigenvectors  $|u(\vec{k}, n)\rangle = \exp(-i\vec{k} \cdot \hat{r}) |\psi(\vec{k}, n)\rangle$ . It is this connexion which naturally occurs in the expression (1.24) : it should not be confused with other "projected" connexions which can be defined in terms of Bloch eigenstates [16, 27].

Following Sundaram and Niu [58], we write down a classical Lagrangian

$$\mathcal{L} = \langle \psi_{\vec{r}_c, \vec{k}_c}^{(n)} | i\hbar \partial_t | \psi_{\vec{r}_c, \vec{k}_c}^{(n)} \rangle - \langle \psi_{\vec{r}_c, \vec{k}_c}^{(n)} | H | \psi_{\vec{r}_c, \vec{k}_c}^{(n)} \rangle, \quad (1.25)$$

with

$$\langle \psi_{\vec{r}_c, \vec{k}_c}^{(n)} | i\hbar \partial_t | \psi_{\vec{r}_c, \vec{k}_c}^{(n)} \rangle = \frac{e}{c} \vec{r}_c \cdot \frac{d\vec{A}(\vec{r}_c)}{dt} + \hbar \vec{k}_c \cdot \frac{d\vec{r}_c}{dt} + \hbar \frac{d\vec{k}_c}{dt} \cdot \vec{A}^{(n)}(\vec{k}_c) \quad (1.26)$$

$$\langle \psi_{\vec{r}_c, \vec{k}_c}^{(n)} | H | \psi_{\vec{r}_c, \vec{k}_c}^{(n)} \rangle = \epsilon(\vec{k}_c) - \vec{B} \cdot \vec{m}(\vec{k}_c) - eV(\vec{r}_c), \quad (1.27)$$

where  $\vec{m}(\vec{k}_c)$  is an orbital magnetic moment [67], which is neglected below. The Lagrange equations on  $\mathcal{L}$  provide the required classical equations of motion :

$$\hbar \frac{d\vec{k}_c}{dt} = -e\vec{E} - \frac{e}{c} \frac{d\vec{r}_c}{dt} \times \vec{B}(\vec{r}_c) \quad \text{with } \vec{B} = \vec{\nabla}_{\vec{r}} \times \vec{A}(\vec{r}) \quad (1.28)$$

$$\frac{d\vec{r}_c}{dt} = \frac{1}{\hbar} \vec{\nabla}_{\vec{k}} \epsilon(\vec{k}_c) - \frac{d\vec{k}_c}{dt} \times \vec{\mathcal{F}}(\vec{k}_c) \quad \text{with } \vec{\mathcal{F}}(\vec{k}_c) = \vec{\nabla}_{\vec{k}} \times \vec{A}(\vec{k}_c). \quad (1.29)$$

Note that in the presence of time-reversal symmetry, the Berry curvature  $\vec{\mathcal{F}}(\vec{k}_c)$  vanishes and we recover the standard classical equation of motion in a crystal. Focusing on situations in the absence of a magnetic field, we will thus forget these Berry terms in the following.

*Linear homogeneous response.* We focus on the charge response of Dirac surface states to a homogeneous field: this amounts to consider the homogeneous solutions  $f(\vec{p}_c = \hbar\vec{k}_c, t)$  of the equation (1.21). This simplification does not hold when considering e.g. the thermoelectric current with a spatially varying temperature. In the homogeneous case, the collision integral occurring in equation (1.21) is simply defined as

$$I[f] = \int \frac{d^2\vec{k}'}{(2\pi)^2} \left[ f(\vec{k}') (1 - f(\vec{k})) - f(\vec{k}) (1 - f(\vec{k}')) \right] \mathcal{M}(\vec{k}, \vec{k}') \quad (1.30)$$

$$= \int \frac{d^2\vec{k}'}{(2\pi)^2} \left[ f(\vec{k}') - f(\vec{k}) \right] \mathcal{M}(\vec{k}, \vec{k}'), \quad (1.31)$$

where  $\mathcal{M}(\vec{k}, \vec{k}')$  is a transition amplitude specified below in eq. (1.38). By definition, the equilibrium distribution which is stationary without any external perturbing field, satisfies  $I[f_{eq}] = 0$ . Within linear response theory, we expand the stationary homogeneous distribution to first order in the perturbing field  $\vec{E}$  around the equilibrium distribution :

$$f(\vec{k}) = f_{eq}(\vec{k}) + f^{(1)}(\vec{k}), \quad (1.32)$$

where  $f_{eq}(\vec{k}) = n_F(\epsilon(\vec{k}) - \epsilon_F)$  where  $n_F, \epsilon_F$  are respectively the Fermi-Dirac distribution function and Fermi energy. Here and in the following we use the simpler notation  $\vec{k}$  for the momentum parametrizing the semi-classical wave-packet. The Boltzmann equation then simplifies into  $-e\vec{E} \cdot \vec{\nabla}_{\vec{k}} f = I[f]$ . The linearity in  $f$  of eq.(1.31) allows to write to lowest order in  $\vec{E}$  :

$$-e\vec{E} \cdot \vec{\nabla}_{\vec{k}} f_{eq} = I[f^{(1)}]. \quad (1.33)$$

*Transport time approximation.* The standard transport time ansatz for a solution of the Boltzmann equation (1.21) amounts to replace the collision integral (1.31) by  $I[f] = \tau_{tr}^{-1} f$  : if the external field  $\vec{E}$  driving the system out-of-equilibrium is turned off,  $\tau_{tr}$  describes the characteristic time of relaxation towards equilibrium of the distribution  $f$ . We will discuss below the validity of this ansatz. Introducing the group velocity  $\vec{v}(\vec{k}) = \vec{\nabla}_{\vec{k}} \epsilon(\vec{k})$ , we can rewrite the equation (1.33) using the transport time ansatz as

$$f^{(1)}(\vec{k}) = -e\vec{E} \cdot (\vec{v}(\vec{k})\tau_{tr}) \partial_{\epsilon} n_F(\epsilon(\vec{k})) \simeq e\vec{E} \cdot \vec{\Lambda}_{tr}(\vec{k}) \delta(\epsilon(\vec{k}) - \epsilon_F), \quad (1.34)$$

where we introduced the vector transport lengths  $\vec{\Lambda}_{tr}$  [55–57]. The equation (1.34) expresses that the transport time ansatz accounts for the application of an electric field  $\vec{E}$  by a translation of the Fermi surface according to

$$f(\vec{k}) = f_{eq}(\vec{k}) - \frac{e\tau_{tr}}{\hbar} \vec{E} \cdot \vec{\nabla}_{\vec{k}} f_{eq} \simeq f_{eq} \left( \vec{k} - \frac{e\tau_{tr}}{\hbar} \vec{E} \right) = n_F \left( \epsilon(\vec{k}) + e\vec{\Lambda}_{tr}(\vec{k}) \cdot \vec{E} \right). \quad (1.35)$$

For an isotropic Fermi surface, it is natural to expect the response to a homogenous electric field  $\vec{E}$  to be independent of the direction of application : a single transport time is necessary to describe this response. However, for an anisotropic Fermi surface

## 12 Transport of Dirac Surface States

with several symmetry axis, we expect different transport times or transport vectors  $\vec{\Lambda}(\vec{k}, \vec{E})$  to be necessary to describe the response to different orientations of the applied electric field with respect to the Fermi surface. This is the case for the hexagonally warped Fermi surface occurring e.g. in  $\text{Bi}_2\text{Te}_3$  and introduced in eq.(1.4), as described in [3]. Note that this anisotropy of the Fermi surface leading to the existence of different transport vectors should not be confused with the anisotropy of scattering by disorder which manifests itself as a discrepancy between transport and elastic mean free time. In the case of Dirac surface states, the scattering is anisotropic, but the Fermi surface remains isotropic when warping is neglected.

*Conductivity.* The current density can be deduced from (1.35) by using  $\vec{j} = e \int d^2\vec{k} (f(\vec{k}) - f_{eq}(\vec{k}))\vec{v}(\vec{k})$ . The conductivity tensor  $\sigma_{\alpha\beta}$  defined by  $j_\alpha = \sigma_{\alpha\beta} E_\beta$  satisfies Einstein relation  $\sigma_{\alpha\beta} = e^2 \rho(\epsilon_F) D_\alpha \delta_{\alpha\beta}$ . To express the diffusion coefficients  $D_\alpha$  we introduce the coordinate  $k_\parallel$  along constant energy contours and  $\rho(\epsilon, k_\parallel)$  the corresponding density of states satisfying  $d^2\vec{k}/(2\pi)^2 = \rho(\epsilon, k_\parallel) d\epsilon dk_\parallel$ . We obtain

$$D_\alpha = \frac{1}{\rho(\epsilon_F)} \oint dk_\parallel \rho(\epsilon_F, k_\parallel) v_\alpha(k_\parallel) \Lambda_\alpha(k_\parallel). \quad (1.36)$$

In the case of an isotropic two dimensional Fermi surface we recover the usual form  $D_x = D_y = D = \tau_{tr} v_F^2/2$ , corresponding to

$$\sigma_{xx}(\epsilon) = e^2 \rho(\epsilon_F) \frac{\tau_{tr} v_F^2}{2} = \frac{e^2}{h} \frac{\epsilon_F}{2} \frac{\tau_{tr}}{h}, \quad (1.37)$$

with :  $\rho(\epsilon_F) = \epsilon_F/(2\pi\hbar^2 v_F^2)$  for Dirac fermions as opposed to  $\rho(\epsilon) = m/(2\pi\hbar^2)$  and  $\sigma = (e^2/h)(v_F^2 \tau m/\hbar)$  for parabolic bands.

*Transport Time.* The conductivity depends on the phenomenological transport time in (1.37) that we will now express in terms of the amplitude of the scattering potential. Using the Born approximation the transition amplitude of scattering is expressed in terms of the matrix elements of the disorder potential introduced in (1.6) :

$$\mathcal{M}(\vec{k}, \vec{k}') = \frac{2\pi}{\hbar} \left\langle |\langle \vec{k} | V | \vec{k}' \rangle|^2 \right\rangle_V \delta(\epsilon(\vec{k}) - \epsilon(\vec{k}')). \quad (1.38)$$

The corresponding collision integral (1.31) satisfies the required condition  $I[f_{eq}] = 0$  for any equilibrium distribution parametrized by the energy  $f_{eq}(\epsilon(\vec{k}))$ . In eq. (1.6), we identify a contribution specific to the Dirac fermion originating from the last term, which expresses a strong backscattering reduction : scattering is much less efficient for Dirac fermions than for non-relativistic electrons. This property is a signature of time-reversal symmetry for a single Dirac cone : the states  $|\psi(\vec{k})\rangle$  and  $|\psi(-\vec{k})\rangle$  carry a spin  $\frac{1}{2}$  and constitute a Kramers pair: they are thus orthogonal. This property implies that scattering for Dirac fermions is intrinsically anisotropic : we thus have to resort to the standard description of transport properties in the presence of anisotropic scattering. Let us plug back the expression (1.38) in the Boltzmann equation (1.33) with the transport time ansatz :

$$-e\vec{E}\cdot\vec{v}(\vec{k})\delta(\epsilon(\vec{k})-\epsilon_F)=I[f^{(1)}]=\frac{1}{\tau_{tr}}f^{(1)}(\vec{k}) \quad (1.39)$$

$$\Rightarrow\frac{\hbar}{\tau_{tr}}=2\pi\int d\theta'\rho(\epsilon_F,\theta')[1-\hat{v}(\theta)\cdot\hat{v}(\theta')]\cos^2\left(\frac{\theta-\theta'}{2}\right)\gamma_V(\epsilon_F,\theta,\theta'). \quad (1.40)$$

For Dirac fermions  $\hat{v}(\theta)\cdot\hat{v}(\theta')=\cos(\theta-\theta')$ : we obtain for an isotropic Dirac Fermi sea  $\rho(\epsilon_F,\theta)=\rho(\epsilon_F)/(2\pi)$  and a transport time independent on the incident direction:

$$\frac{\hbar}{\tau_{tr}}=\rho(\epsilon_F)\int d\theta'\frac{1-\cos^2\theta'}{2}\gamma_V(\epsilon_F,\theta'). \quad (1.41)$$

The disorder amplitude  $\gamma_V$  was defined in eqs. (1.5,1.6). This expression of the transport time has to be contrasted with the definition of the elastic scattering time which enters e.g. in the Dingle factor for Shubnikov - de Haas oscillations :

$$\frac{\hbar}{\tau_e}=\rho(\epsilon_F)\int d\theta'\gamma_V(\epsilon_F,\theta'). \quad (1.42)$$

The discrepancy between the transport and elastic scattering times is a consequence of the anisotropic nature of scattering, which originates in the nature of the Dirac fermions in the present case. For an isotropic disorder for which  $\gamma_V(\epsilon_F,\theta)=\gamma_V(\epsilon_F)$  independent of  $\theta$ , we recover the standard result  $\tau_{tr}=2\tau_e$  : it takes twice longer for Dirac fermions to diffuse isotropically than for conventional electrons.

Note that the expression (1.41) also implies that

$$\sigma=\frac{e^2v_F^2}{2}\rho(\epsilon_F)\tau_{tr}\text{ with } \rho(\epsilon_F)\tau_{tr}=\frac{2\hbar}{\pi\gamma_V(\epsilon_F)}. \quad (1.43)$$

As a consequence of this result, for Dirac fermions in the classical regime the energy dependance of the Boltzmann conductivity originates only from the disorder correlations. Corrections to this behavior can be attributed to a renormalization of the density requiring a self-consistent treatment beyond the Born approximation [38], or to quantum corrections described below.

### 1.3.2 Linear Response Approach

We aim at recovering the previous classical conductivity for the Dirac fermions within a linear response approach which allows later to incorporate quantum corrections. We start from the Kubo formula, introduced in section 1.2.3 when studying the minimal conductivity at the Dirac point.

*Kubo formula.* We consider the longitudinal conductivity  $\sigma=\sigma_{xx}$  of a sample of typical size  $L$ . This conductivity is calculated within linear response theory from the Kubo formula introduced in equation (1.17) in terms of the Green's function defined in eq. (1.18). Focusing on the zero temperature and  $\omega=0$  longitudinal conductivity, we can focus on the expression

$$\sigma=\frac{\hbar}{2\pi L^2}\text{ReTr}\left(\hat{j}_x\hat{\mathcal{G}}^R(\epsilon_F)\hat{j}_x\hat{\mathcal{G}}^A(\epsilon_F)\right) \quad (1.44)$$

where the trace runs over the quantum numbers (spin and momentum) of electronic states and we have neglected contribution  $\propto\mathcal{G}^R\mathcal{G}^R,\mathcal{G}^A\mathcal{G}^A$  which are systematically

## 14 Transport of Dirac Surface States

of lower order than the terms we have kept in the following perturbative expansion in  $1/k_F l_e$  [4]. This conductivity depends on disorder through the Green's functions (1.18). We focus on the diffusive regime, corresponding to the semi-classical regime where  $\lambda_F$  is small compared to the mean scattering length  $l_e$ . The natural small parameter is  $1/(k_F l_e)$ . In this regime, we don't expect the conductivity to depend on the exact configuration of disorder, but only on its strength. Such a quantity is called a self-averaging observable: its typical value identifies with its average over disorder configurations which is easier to calculate.

Working perturbatively in the disorder allows to expand the retarded and advanced Green's functions following

$$\hat{\mathcal{G}}^R = [(\hat{\mathcal{G}}_0^R)^{-1} - V]^{-1} = \hat{\mathcal{G}}_0^R \sum_{n=0}^{\infty} (V \hat{\mathcal{G}}_0^R)^n, \quad (1.45)$$

where the Green's functions for the pure Hamiltonian are defined in eq. (1.19) with  $\tau = \tau_\phi$  and no disorder potential. Averaging any combination of these Green's functions over a gaussian distribution for  $V$  amounts to pair all occurrences of the disorder potential  $V$ . When performing this task on the conductivity (1.44), two different pairings appear : the first consists in pairing potentials  $V$  within the expansion of  $\hat{\mathcal{G}}^R$  and  $\hat{\mathcal{G}}^A$  independently from each other, and the second pairing occurrences of  $V$  in the expansion of  $\hat{\mathcal{G}}^R$  with occurrences in the expansion of  $\hat{\mathcal{G}}^A$ . The former amounts to replace  $\hat{\mathcal{G}}^R$  and  $\hat{\mathcal{G}}^A$  by their average over disorder, while the latter corresponds to the cooperon and diffuson contributions discussed below.

*Averaged Green's function and self-energy.* Averaging the expansion (1.45) over disorder can be accounted for by introducing a self energy  $\Sigma$  defined as

$$\langle \hat{\mathcal{G}}^R \rangle_V^{-1} = \hat{\mathcal{G}}_0^{-1} - \Sigma, \quad (1.46)$$

where to lowest order in  $\gamma_V$

$$\Sigma(\epsilon) = \int \frac{d\vec{k}'}{(2\pi)^2} \langle V(\vec{k}') V(-\vec{k}') \rangle_V \mathcal{G}_0^R(\vec{k} - \vec{k}', \epsilon) = \gamma_V \int \frac{d^2 \vec{k}}{(2\pi)^2} \mathcal{G}_0^R(\vec{k}, \epsilon). \quad (1.47)$$

The real part of this self-energy is incorporated in a redefinition of the arbitrary origin of energies while its imaginary part defines the elastic scattering time

$$-\text{Im}(\Sigma) = \frac{\hbar}{2\tau_e} = \pi \gamma_V \rho(\epsilon_F). \quad (1.48)$$

Hence, the averaging procedure of the Green's function amounts to replace the dephasing rate of the bare Green's function by :  $\tau_\phi^{-1} \rightarrow \tau_\phi^{-1} + \tau_e^{-1}$ . In practice,  $\tau_\phi^{-1}$  is often negligible compared to  $\tau_e^{-1}$  in this Mathiessen rule and averaged Green's functions are simply given by (1.19) with  $\tau = \tau_e$ . We can now use these expressions in the average of the Kubo expression (1.44) by approximating  $\langle \mathcal{G}^R \mathcal{G}^A \rangle_V$  by the product of averages

$\langle \mathcal{G}^R \rangle_V \langle \mathcal{G}^A \rangle_V$ . Performing the remaining trace we recover an Einstein formula for the conductivity

$$\langle \sigma \rangle_0 = \frac{v_F^2 \tau_e}{2} = D_0 e^2 \rho(E_F), \quad (1.49)$$

but with a diffusion coefficient  $D_0$  which is half the correct Boltzmann expression (1.37). This discrepancy is the consequence of the inherent anisotropy of scattering for Dirac fermions, which manifests itself in the difference between the transport and elastic scattering times. In the present perturbative expansion, it occurs as the contribution of an additional class of diagrams.

*The dominant contributions : cooperon and diffuson.* Standard diagrammatic theory of the diffusive regime amounts to sum an infinite set of dominant diagrams perturbative in disorder strength [37]. These contributions are conveniently represented by the diffusive propagation of pseudo-particles, the co-called diffusons and cooperons (see [4] for a recent pedagogical presentation). We can resort to a simple physical argument to gain an intuitive understanding of the origin of these contributions. This is most con-

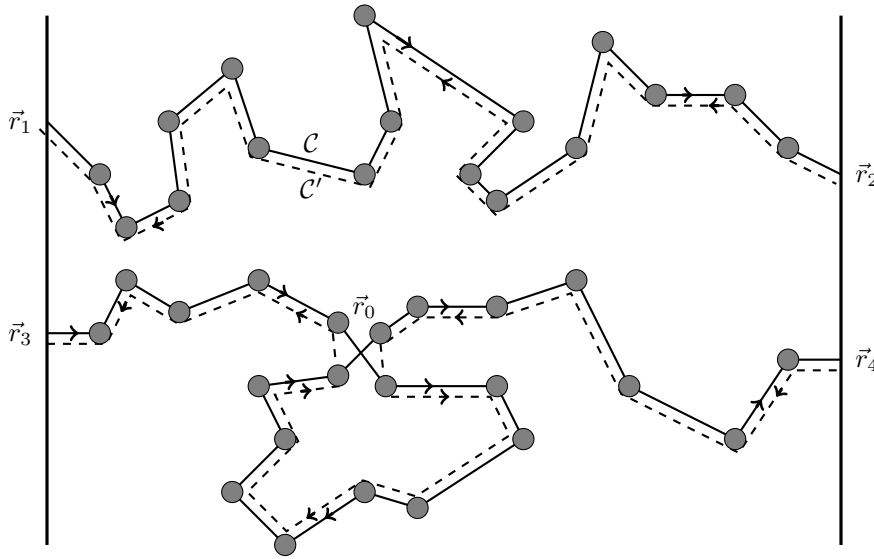


**Fig. 1.3** On the top : contribution corresponding to an electron and hole moving along the same path  $\mathcal{C} = \mathcal{C}'$ , denoted as the propagation of a diffuson. (Bottom) : contribution corresponding to an electron-like and hole-like excitation moving in opposite directions along a loop of the path. Along this loop, this correspond to the propagation of two particles in the same direction, accounted for by the diffusive propagation of a cooperon. Note that in this last case, quantum crossing between paths occurs at point  $\vec{r}_0$ .

veniently done by considering the probability to transfer an electron across the sample from position  $\vec{r}_1$  to  $\vec{r}_2$ , which is tightly related with the conductivity. In a semi-classical description, this probability is related to the amplitude  $\mathcal{A}_{\vec{r}_1 \vec{r}_2}$  of diffusion from  $\vec{r}_1$  to

$\vec{r}_2$ , which itself can be summed *à la Feynman* over contributions labeled by classical diffusive paths :

$$P(\vec{r}_1, \vec{r}_2) = |\mathcal{A}_{\vec{r}_1 \vec{r}_2}|^2 = \left| \sum_{\mathcal{C}: \vec{r}_1 \rightarrow \vec{r}_2} \mathcal{A}_{\mathcal{C}} \right|^2 = \sum_{\mathcal{C}, \mathcal{C}'} \mathcal{A}_{\mathcal{C}} \mathcal{A}_{\mathcal{C}'}^*, \quad (1.50)$$

where  $\mathcal{C}$  and  $\mathcal{C}'$  are two diffusive paths (or scattering sequences for discrete impurities), from  $\vec{r}_1$  to  $\vec{r}_2$ .  $\mathcal{A}_{\mathcal{C}}, \mathcal{A}_{\mathcal{C}'}$  represent the corresponding diffusion amplitudes along these paths. Note that we can view  $\mathcal{A}_{\mathcal{C}'}^*$  as the amplitude of diffusion for a hole in the Fermi sea.

Electrons are described in point  $\vec{r}_1$  by a Bloch state, and when evolving along a given path  $\mathcal{C}$  their phase is incremented by  $k_F \mathcal{L}(\mathcal{C})$  where  $\mathcal{L}(\mathcal{C})$  is the length of  $\mathcal{C}$  (we neglect any geometrical Berry contribution in this argument). In a good metal, which is the situation considered in this section, the fermi wavelength  $2\pi/k_F$  is typically of order of the crystal lattice constant. Hence this phase  $k_F \mathcal{L}(\mathcal{C})$  varies of order of  $2\pi$  as soon as the path is modified over a (few) lattice spacing(s). Hence, for two different paths  $\mathcal{C} \neq \mathcal{C}'$ , the relative phase  $\mathcal{L}(\mathcal{C}) - \mathcal{L}(\mathcal{C}')$  appearing in eq. (1.50) will vary by  $2\pi$  over neighboring paths for which the amplitude  $|\mathcal{A}_{\mathcal{C}} \mathcal{A}_{\mathcal{C}'}^*|$  can be assumed constant. Hence this term will vanish upon the summation over the paths  $\mathcal{C}, \mathcal{C}'$  (corresponding to a disorder average). The only term surviving this summation are those for which  $\mathcal{L}(\mathcal{C}) = \mathcal{L}(\mathcal{C}')$ . This property is naturally associated with pairs of identical paths  $\mathcal{C} = \mathcal{C}'$  which can be viewed as the propagation of an electron and a hole correlated by the disorder: this statistical coupling of path by disorder is conveniently viewed as the propagation of a pseudo-particle called a *diffuson*. A second solution exists for a path  $\mathcal{C}$  containing a loop : see figure 1.3 (bottom part). In this case, the path  $\mathcal{C}'$  identifies with  $\mathcal{C}$  except around the loop along which the direction of propagation is reversed.  $\mathcal{C}'$  possesses approximatively the same length as  $\mathcal{C}$ . The corresponding contribution can be viewed as the diffusion of a diffuson up to and from the loop, and the counter propagation of a particle and hole around the loop. This counter propagation is also interpreted as the correlated propagation of two particles along the same loop and called a *cooperon* by analogy with Cooper pairs in superconductors. The existence of the cooperon is tightly related to the time-reversal symmetry of transport which identifies the amplitudes  $\mathcal{A}_{\mathcal{C}'}$  with  $\mathcal{A}_{\mathcal{C}}$  : it will disappear upon application of a small magnetic field. Note that on the bottom part of figure 1.3, a crossing of paths appears when drawing the reconnection of a diffuson with a cooperon. The number of such crossings will turn out to be the correct parameter for the perturbative theory.

*Classical or Quantum ?* In the presence of a dynamic environment accounting for the inelastic interaction of the propagating electrons with other electrons, phonons, etc, we realize that the contribution corresponding to the diffuson is not affected : both the electron and the hole contribution encounter the same environment during their evolution, and are not dephased with respect to each other. Their possible interference contributions are not affected by this fluctuating environment : this is the signature of a classical contribution. On the other hand the cooperon contribution corresponds to an electron and a hole propagating in opposite directions along the loop

$$\text{————} = \langle \mathcal{G}^R \rangle_V \quad \text{-----} = \langle \mathcal{G}^A \rangle_V \quad \begin{array}{c} \bullet \\ \vdots \\ \text{---} \end{array} = \langle V^2 \rangle_V$$

**Fig. 1.4** Conventions for the diagrammatic perturbative theory.

$$\begin{array}{c} \Gamma \\ \hline \end{array} = \begin{array}{c} \text{---} \\ \bullet \\ \text{---} \\ \vdots \\ \text{---} \end{array} + \begin{array}{c} \text{---} \\ \bullet \quad \bullet \\ \text{---} \\ \vdots \\ \text{---} \end{array} + \begin{array}{c} \text{---} \\ \bullet \quad \bullet \quad \bullet \\ \text{---} \\ \vdots \\ \text{---} \end{array} + \begin{array}{c} \text{---} \\ \bullet \quad \bullet \quad \bullet \quad \bullet \\ \text{---} \\ \vdots \\ \text{---} \end{array} + \dots$$

$$\begin{array}{c} \vec{k} + \frac{\vec{q}}{2} \\ \alpha \\ \hline \Gamma_{\alpha\beta,\gamma\delta}(\vec{q}) \\ \hline \beta \\ \vec{k} - \frac{\vec{q}}{2} \end{array} = \begin{array}{c} \vec{k}' + \frac{\vec{q}}{2} \\ \alpha \\ \hline \bullet \\ \hline \beta \\ \vec{k}' - \frac{\vec{q}}{2} \end{array} + \begin{array}{c} \vec{k} + \frac{\vec{q}}{2} \\ \alpha \\ \hline \Gamma_{\alpha\beta,\mu\nu}(\vec{q}) \\ \hline \beta \\ \vec{k} - \frac{\vec{q}}{2} \end{array} \begin{array}{c} \vec{k}' + \frac{\vec{q}}{2} + \vec{q}_1 \\ \gamma \\ \hline \mu \\ \vec{k}' - \frac{\vec{q}}{2} + \vec{q}_1 \\ \hline \nu \\ \vec{k}' - \frac{\vec{q}}{2} \\ \delta \end{array}$$

**Fig. 1.5** Diagrammatic representation of the recursive calculation satisfied by the diffuson structure factor.

: they encounter different dynamical environment during their propagation, and are dephased with respect to each other during this evolution. This is the manifestation of a quantum contribution : we expect the cooperon contribution to correspond to loops of length smaller than the typical dephasing length  $L_\phi$  (with  $L_\phi^2 \simeq D\tau_\phi$ ). When we will study the conductivity fluctuations, we will encounter different cooperon and diffuson which correspond to the propagation correlated by the disorder of a particle and a hole evolving in different thermal environment : in this situation, both cooperon and diffuson are affected by a dephasing due to their environment, and correspond to quantum corrections to the conductivity fluctuations.

*Diffuson contribution to the conductivity.* Let us for now focus on the classical contribution to the conductivity. For simplicity in the following we will consider a Dirac cone without warping (see [3] for a non perturbative treatment of warping using the diagrammatic formalism). According to the previous discussion, the correction to the expression (1.49) of the conductivity comes from contributions of the diffuson (top part of figure 1.3). The corresponding term requires the summation over a geometric series of diagrams of same perturbative order [37, 4]. It is best represented diagrammatically: we will use the convention of figure 1.4 to represent averaged Green's function and disorder correlations (second cumulant). The real space picture of the diffuson contribution can be represented as a contribution to the conductivity : it corresponds to the insertion in the trace occurring in the Kubo formula (1.44) of a sequence (diffusion path) of retarded and advanced Green's function representing the evolution of a particle and hole, correlated by the disorder. It turns out that sequences (or path) of all lengths contribute to the final result : the summation over all sequences amounts to consider a "diffuson structure factor"  $\Gamma$  obtained from the algebraic sum of terms shown in figure 1.5.

## 18 Transport of Dirac Surface States

The recursive nature of this algebraic sum represented in figure 1.5 can be expressed by the relation

$$\Gamma_{\alpha\beta,\gamma\delta}(\vec{q}) = \gamma_V \mathbf{I}_{\alpha\gamma} \otimes \mathbf{I}_{\beta\delta} + \gamma_V \Gamma_{\alpha\beta,\mu\nu}(\vec{q}) \Pi_{\mu\nu,\gamma\delta}(\vec{q}), \quad (1.51)$$

where we have explicitly written the dependance on spin indices, and  $\Pi$  is the quantum diffusion probability [4] :

$$\Pi_{\mu\nu,\gamma\delta}(\vec{q}) = \frac{1}{L^2} \sum_{\vec{q}_1} \langle \mathcal{G}_{\mu\gamma}^R(\vec{q}_1 + \vec{q}) \rangle_V \langle \mathcal{G}_{\nu\delta}^A(\vec{q}_1) \rangle_V. \quad (1.52)$$

By using the expression (1.19) for the Green's functions we can perform the integral over momentum in the diffusive limit and obtain

$$\begin{aligned} \Pi(\vec{q}) = \frac{1}{2\gamma_V} \left[ (1 - 2w_e^2) \mathbf{I} \otimes \mathbf{I} + \frac{1}{2} (1 - w_e^2) \vec{\sigma} \otimes \vec{\sigma} \right. \\ \left. - iw_e (\hat{q} \cdot \vec{\sigma} \otimes \mathbf{I} + \mathbf{I} \otimes \hat{q} \cdot \vec{\sigma}) - w_e^2 \hat{q} \cdot \vec{\sigma} \otimes \hat{q} \cdot \vec{\sigma} \right] + \mathcal{O}(w_e^2), \quad (1.53) \end{aligned}$$

with  $w_e = \tau_e v_f q / 2 \ll 1$  in the diffusive limit and we used the notation  $\vec{\sigma} = (\sigma_x, \sigma_y)$ ,  $\hat{q} = \vec{q}/|q|$ . Note that in the present case, the "complexity" of the structure factor  $\Gamma$ , *i.e.* its spin content, originates from the free Green's functions of the Dirac particles embedded in the probability  $\Pi$  and not the symmetry of the disorder correlations  $\gamma_V$  as is standard for quadratic bands [4].

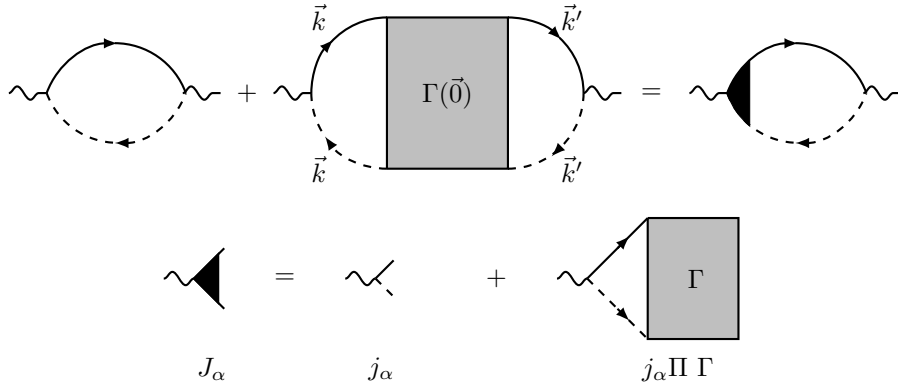


**Fig. 1.6** Diagrammatic representation of the bare and diffuson contributions to the averaged conductivity (top) and of the renormalization of the vertex current operator accounting for the contribution of the diffuson (bottom).

The sum of the bare and diffuson contribution to the conductivity represented in Fig. 1.6 are expressed as

$$\sigma = \frac{\hbar}{2\pi L^2} \text{ReTr} [j_x \Pi j_x] + \frac{\hbar}{2\pi L^2} \text{ReTr} [j_x \Pi \Gamma \Pi j_x], \quad (1.54)$$

where we use the condensed notation for the spin contractions :  $\text{Tr} [j_x \Pi j_x] = j_{\beta\alpha} \Pi_{\alpha\beta, \gamma\delta} j_{\gamma\delta}$ . These two contributions can be recast as a modification or renormalization of the vertex current operator using the equation (1.51), written in condensed form as  $\gamma_V^{-1} \Gamma = \mathbf{I} + \Gamma \Pi$  :

$$\sigma = \frac{\hbar}{2\pi L^2} \gamma_V^{-1} \text{ReTr} [j_x \Pi \Gamma j_x] = \frac{\hbar}{2\pi L^2} \text{ReTr} [j_x \Pi J_x], \quad (1.55)$$

with the ‘‘renormalized’’ vertex current operator represented on figure 1.6 and defined by

$$J_x = j_x + \Gamma \Pi j_x = \gamma_V^{-1} \Gamma j_x. \quad (1.56)$$

Note that only the limit  $\vec{q} \rightarrow \vec{0}$  of  $\Pi(\vec{q})$  enters this expression, which from eq. (1.53) reduces to

$$\Pi(\vec{q} = \vec{0}) = \frac{1}{2\gamma_V} \left[ \mathbf{I} \otimes \mathbf{I} + \frac{1}{2} \sigma_x \otimes \sigma_x + \frac{1}{2} \sigma_y \otimes \sigma_y \right]. \quad (1.57)$$

From this expression, we obtain the renormalized vertex

$$J_\alpha = (ev_F) \gamma_V^{-1} \Gamma(\vec{q} = \vec{0}) \sigma_\alpha \quad (1.58)$$

$$= (ev_F) \left[ \mathbf{I} \otimes \mathbf{I} - \gamma_V \Pi(\vec{q} = \vec{0}) \right]^{-1} \sigma_\alpha \quad (1.59)$$

$$= (ev_F) 2 \left[ \mathbf{I} \otimes \mathbf{I} - \frac{1}{2} \sigma_x \otimes \sigma_x - \frac{1}{2} \sigma_y \otimes \sigma_y \right]^{-1} \sigma_\alpha \quad (1.60)$$

$$= 2(ev_F) \sigma_\alpha = 2j_\alpha \text{ for } \alpha = x, y. \quad (1.61)$$

The final contraction can be done without further algebra: we obtain twice the result of eq. (1.49). This result correspond to a renormalization by 2 of the current operator :  $J_\alpha = 2j_\alpha$ . Hence we recover the Boltzmann result of eq. (1.43) : the anisotropic scattering inherent to the Dirac nature of the particles leads to a doubling of the transport time with respect to the elastic scattering time.

Note that the notation of equation (1.59) is misleading and should be read as  $J_\alpha = (ev_F) \gamma_V^{-1} \lim_{q \rightarrow 0} \Gamma(\vec{q}) \sigma_\alpha$ . Indeed from the discussion around Fig. 1.3 we expect  $\Gamma(\vec{q})$  to possess long wavelengths diffusive modes, corresponding to eigenenergies  $\simeq 1/(Dq^2)$  of  $\Gamma(\vec{q})$ . These diffusive modes encode the quantum corrections to transport. As a consequence, in the limit  $\vec{q} \rightarrow \vec{0}$  the operator  $\mathbf{I} - \gamma_V \Pi(\vec{q})$  is no longer invertible and  $\Gamma(\vec{q})$  becomes ill defined. However we can explicitly check that the contraction  $\Gamma(\vec{q}) \cdot \sigma_\alpha$  remains well defined in this limit, which justifies *a posteriori* the above notation. Indeed, the renormalization of elastic scattering time into a transport time occurs on short distance, and is expected to be independent from the long distance physics of the diffusive quantum modes. This is demonstrated by the above property: the vertex renormalization of eq.(1.59) does not depends on the vanishing modes of  $\mathbf{I} - \gamma_V \Pi(\vec{q})$ , but only on its (non universal) massive modes.

## 1.4 Quantum transport of Dirac fermions

The last three decades have seen the exploration of electronic transport in conductors below the micrometer scale [9, 18]. Due to the interaction with its environment the phase  $\phi$  of an electron is randomly incremented during its evolution: this phase evolution on the unit circle is characterized by the rate of increase of the fluctuations  $\overline{(\delta\phi)^2}$ . As the electron evolves in real space, its phase  $\phi$  spreads over the unit circle. Beyond a characteristic length  $L_\phi$ , the variance of the phase is of order  $\overline{(\delta\phi)^2} \simeq (2\pi)^2$ : the statistical uncertainty on the electron phase due to the coupling with the environment forbids any measurable interference effect. By lowering the temperature (density of phonons), we increase the corresponding phase coherence length  $L_\phi(T)$  for the electrons (at lower temperatures, other mechanisms such as electron-electron interactions and the Kondo effects on magnetic impurities take over). At temperatures  $T \simeq 100mK$  the typical order of magnitude of  $L_\phi(T)$  is a few  $\mu m$ . The study of such small conductors at low temperature has led to the appearance of a new domain of research: the mesoscopic quantum physics [9, 18]. Many features of transport of such mesoscopic conductors are remarkable: the quantum corrections to the conductance of a mesoscopic conductor depend on the precise locations of impurities in a given sample: different mesoscopic samples prepared in exactly the same protocol (or successive annealing of a given sample allowing for disorder reorganizations) display different values of conductance. In this regime the phase-coherent conductance is said to be a non self-averaging observable: it fluctuates from sample to sample for sizes  $L \leq L_\phi(T)$ . In the limit  $L \gg L_\phi(T)$ , the conductor can be viewed as an incoherent collection of pieces of size  $L_\phi(T)$  and relative fluctuations are statistically reduced: we recover the previous classical regime. The description of the conductance of a phase coherent conductor requires the use of a distribution function, which for weak disorder is a gaussian characterized by two cumulants. Moreover the conductance fluctuates as a function of a weak transverse magnetic flux threading the sample. These fluctuations should not be confused with noise: they are perfectly reproducible for a given sample and do not fluctuate in time as typical  $1/f$  noise. Indeed, the whole magneto-conductance trace is modified as the sample is annealed: each curve appears as a unique signature of the impurities location in the sample. It is a real fingerprint of the configuration of disorder.

The origin of this magneto-conductance and its quantum origin can be understood as follows. As hinted in section 1.3.2, along a given diffusive path, the phase of an electronic state is incremented by  $\delta\phi_{\mathcal{L}} = k\mathcal{L}$  where  $\mathcal{L}$  is the length of the path. For electrons at the Fermi level,  $k \simeq k_F$ , and this phase  $\delta\phi_{\mathcal{L}} \simeq 2\pi\mathcal{L}/\lambda_F$  is extremely sensitive on the length  $\mathcal{L}$ , typically much larger than the Fermi wavelength  $\lambda_F$ . Between different samples the positions of these impurities are different, and all the lengths  $\mathcal{L}$  are modified by at least  $\lambda_F$ , and correspondingly the phases  $\delta\phi_{\mathcal{L}}$  are redistributed randomly. The conductivity being a *non self-averaging* quantity, its value is then different from sample to sample. A different procedure allows to redistribute these phases along the diffusive path: the application of a transverse magnetic field. The presence of such a field can be accounted for by an extra dephasing  $e \int_{\mathcal{L}} \mathbf{A} \cdot d\mathbf{l}$  along each path  $\mathcal{L}$ ,  $\mathbf{A}$  being the vector potential. The shape of these paths  $\mathcal{L}$  and thus the associated magnetic phases are random: similarly to a change of impurity positions, the mag-

netic field redistribute the phases associated with each path in a sample and changes accordingly the value of the conductivity. Whenever a new quantum of magnetic flux is added through the sample, the typical phase shift between two paths crossing the sample is of order  $2\pi$ , and we obtain a different value of the conductivity. Moreover this function  $G(B)$ , called a magneto conductance trace, provides an invaluable access to the statistics of conductance in the quantum regime. Since both the magnetic field and the change of disorder amounts to redistribute the phases in a random manner, we expect both perturbations to lead to the same statistics of the conductance. This is the so-called ergodic hypothesis which turns out to be quantitatively valid for the first two moments of the conductivity distribution [61].

Let us now consider the coherent regime of transport, relevant for transport on time scales shorter than the dephasing time  $\tau_\phi(T)$ , defined from the imaginary part  $\hbar/(2\tau_\phi)$  of the self energy for electrons, see eq. (1.18). In this regime, and for weak enough disorder which is the case experimentally, the conductivity is gaussian distributed, and fully characterized by its first two cumulants. The first cumulant  $\langle \delta\sigma \rangle_V$  describes the so-called weak (anti-)localization correction to the averaged conductivity while the second cumulant  $\langle (\delta\sigma)^2 \rangle_V$  is associated to the universal fluctuations of the conductivity from sample to sample or as a function of the magnetic field. We have already guessed in the discussion of the previous section that the origin of these quantum correction to the conductivity lies in the existence of long wavelength statistical correlations conveniently viewed as propagating diffuson and cooperon modes. In the following, we will briefly review the description of the corresponding diagrammatic contributions.

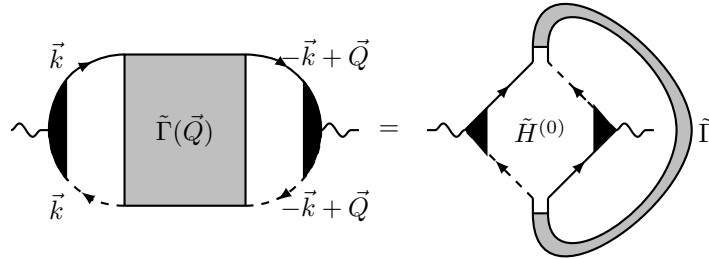
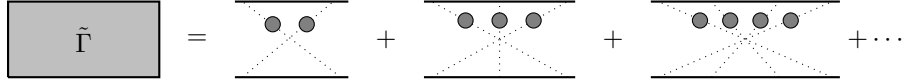


**Fig. 1.7** Diagrammatic representation of the first quantum correction to the averaged conductivity (Left) and equivalent representation in terms of a contraction between a Hikami box and Cooperon structure factor (Right).

#### 1.4.1 Quantum Correction to the conductivity : weak anti-localization

The two contributions represented in figure 1.3 to the average conductivity correspond to diagrams similar to that of Fig.1.6 with either a diffuson or cooperon structure

factor. We have already seen in the previous section that the diffusive mode of the diffuson does not contribute to the average conductivity : only short distance contributions renormalize the vertex operator. Hence we only focus on the contribution of a cooperon structure factor represented in Fig. 1.7 where  $\tilde{\Gamma}$  is a structure factor, analogous to the one in Fig.1.5, and accounting for an infinite series of maximally crossed diagrams :



This series of terms can be recast as a geometric series by time reversal of the advanced branch: similarly than for the diffuson, the cooperon structure factor satisfies a recursive equation:

$$\begin{array}{c}
 \vec{k} + \frac{\vec{Q}}{2} \\
 \alpha \\
 \xrightarrow{\quad} \\
 \tilde{\Gamma}_{\alpha\beta,\gamma\delta}(\vec{Q}) \\
 \xrightarrow{\quad} \\
 -\vec{k} + \frac{\vec{Q}}{2} \\
 \beta
 \end{array}
 =
 \begin{array}{c}
 \alpha \\
 \vdots \\
 \beta
 \end{array}
 +
 \begin{array}{c}
 \vec{k} + \frac{\vec{Q}}{2} \\
 \alpha \\
 \xrightarrow{\quad} \\
 \tilde{\Gamma}_{\alpha\beta,\mu\nu}(\vec{Q}) \\
 \xrightarrow{\quad} \\
 -\vec{k} + \frac{\vec{Q}}{2} \\
 \beta
 \end{array}
 \begin{array}{c}
 \vec{k}' + \frac{\vec{Q}}{2} + \vec{q}_1 \\
 \gamma \\
 \xrightarrow{\quad} \\
 \tilde{\Pi}_{\mu\nu,\gamma\delta}(\vec{Q}) \\
 \xrightarrow{\quad} \\
 -\vec{k}' + \frac{\vec{Q}}{2} \\
 \delta
 \end{array}$$

or equivalently

$$\tilde{\Gamma}_{\alpha\beta,\gamma\delta}(\vec{Q}) = \gamma_V \mathbf{I}_{\alpha\gamma} \otimes \mathbf{I}_{\delta\beta} + \gamma_V \tilde{\Gamma}_{\alpha\beta,\mu\nu}(\vec{Q}) \tilde{\Pi}_{\mu\nu,\gamma\delta}(\vec{Q}), \quad (1.62)$$

with

$$\tilde{\Pi}_{\mu\nu,\gamma\delta}(\vec{Q}) = \frac{1}{V} \sum_{\vec{q}_1} \langle \mathcal{G}_{\mu\gamma}^R(\vec{q}_1) \rangle_V \langle \mathcal{G}_{\nu\delta}^A(\vec{Q} - \vec{q}_1) \rangle_V. \quad (1.63)$$

The value of  $\tilde{\Pi}$  can be deduced by time reversal of the advanced branch of the expression (1.53) of  $\Pi(\vec{q})$ . From inversion of eq. (1.62) we obtain the long wavelength behavior of the cooperon structure factor  $\tilde{\Gamma}(\vec{Q})$ . Only one eigenmode is diffusive with an eigenvalue  $1/(DQ^2)$  for  $Q \rightarrow 0$ , corresponding to a singlet mode. Hence in the diffusive limit the cooperon structure factor reduces to a projector onto this singlet mode :

$$\tilde{\Gamma}(\vec{Q}) = \frac{\gamma_V}{\tau_e} \frac{1}{DQ^2} \frac{1}{4} [\mathbf{I} \otimes \mathbf{I} - \sigma_x \otimes \sigma_x - \sigma_y \otimes \sigma_y - \sigma_z \otimes \sigma_z] \quad (1.64)$$

$$= \frac{\gamma_V}{\tau_e} \frac{1}{DQ^2} |S\rangle\langle S|, \quad (1.65)$$

where  $D$  is the diffusion constant  $D = v_F^2 \tau_e$  and  $|S\rangle$  a singlet state defined in section 1.4.3.

The weak anti-localization correction represented on the left side of Fig. 1.7 is conveniently viewed as a contraction of a cooperon structure factor and a Hikami box, as shown on the right side of Fig. 1.7. The corresponding contribution is

$$\langle \delta\sigma_0 \rangle = \frac{\hbar}{2\pi L^2} \text{Tr} \left[ \mathcal{G}^A(\vec{k}) J_x \mathcal{G}^R(\vec{k}) \tilde{\Gamma}(\vec{Q}) \mathcal{G}^R(\vec{Q} - \vec{k}) J_x \mathcal{G}^A(\vec{Q} - \vec{k}) \right]. \quad (1.66)$$

In this expression, the  $\vec{Q}$  integral (occurring in the trace over quantum numbers) is dominated by the small  $\vec{Q}$  contribution originating from the diffusive pole of the cooperon. This justifies *a posteriori* the projection on the single diffusive mode in (1.64). Focusing on the most dominant part of this expression, we can set  $Q \rightarrow 0$  except in the cooperon propagator, the Green's functions being regular in  $\vec{k}$ : this amounts to set  $\vec{k} = \vec{0}$  in the expression of the Hikami box.

Let us now turn to the expression of this Hikami box: it turns out that besides the contribution depicted in Fig. 1.7, two other terms of the same order have to be included. This is a standard mechanism when scattering is anisotropic [4], and follows from the nature of the Dirac Green's functions. The three contributions consist in considering a renormalized Hikami box as the sum of three terms represented in Fig. 1.8. The

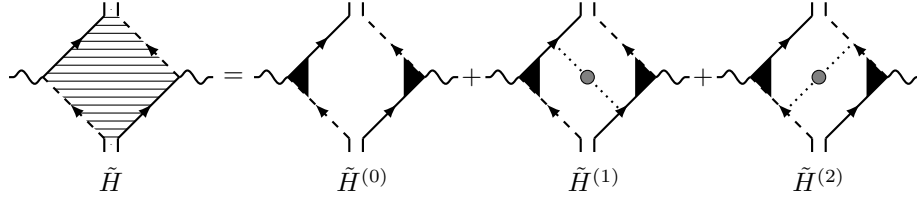


**Fig. 1.8** First renormalized Hikami box as the sum of three contributions.

integrals corresponding to the three terms are performed according to

$$\begin{aligned} \tilde{H}_{xx}^{(0)} &= 4 \int_{\vec{k}} \left[ \mathcal{G}^A(\vec{k}) \sigma_x \mathcal{G}^R(\vec{k}) \right] \otimes \left[ \mathcal{G}^R(-\vec{k}) \sigma_x \mathcal{G}^A(-\vec{k}) \right] \\ &= \rho(\epsilon_F) \left( \frac{2\tau_e}{\hbar} \right)^3 \frac{\pi}{16} [-4 \mathbf{I} \otimes \mathbf{I} + 3 \sigma_x \otimes \sigma_x + \sigma_y \otimes \sigma_y] \end{aligned} \quad (1.67)$$

$$\begin{aligned} \tilde{H}_{xx}^{(1)} &= 4\gamma_V \int_{\vec{k}} \int_{\vec{q}_1} \left[ \mathcal{G}^A(\vec{k}) \sigma_x \mathcal{G}^R(\vec{k}) \mathcal{G}^R(-\vec{q}_1) \right] \otimes \left[ \mathcal{G}^R(-\vec{k}) \mathcal{G}^R(\vec{q}_1) \sigma_x \mathcal{G}^A(\vec{q}_1) \right] \\ &= \frac{\pi}{16} \rho(\epsilon_F) \left( \frac{2\tau_e}{\hbar} \right)^3 [\mathbf{I} \otimes \mathbf{I} - \sigma^x \otimes \sigma^x] \end{aligned} \quad (1.68)$$

$$\begin{aligned} \tilde{H}_{xx}^{(2)} &= 4\gamma_V \int_{\vec{k}} \int_{\vec{q}_1} \left[ \mathcal{G}^A(-\vec{q}_1) \mathcal{G}^A(\vec{k}) \sigma_x \mathcal{G}^R(\vec{k}) \right] \otimes \left[ \mathcal{G}^R(\vec{q}_1) \sigma_x \mathcal{G}^A(\vec{q}_1) \mathcal{G}^A(-\vec{k}) \right] \\ &= \tilde{H}_{xx}^{(1)} \end{aligned} \quad (1.69)$$

Summing these three contributions we obtain the renormalized Hikami box :

$$\tilde{H}_{xx} = \tilde{H}_{xx}^{(0)} + \tilde{H}_{xx}^{(1)} + \tilde{H}_{xx}^{(2)} = \rho(\epsilon_F) \left( \frac{2\tau_e}{\hbar} \right)^3 \frac{\pi}{16} [-2 \mathbf{I} \otimes \mathbf{I} + \sigma^x \otimes \sigma^x + \sigma^y \otimes \sigma^y]. \quad (1.70)$$

The resulting weak anti localization correction is obtained *via* the final contraction with a cooperon structure factor (1.64) as shown on Fig.1.7 (with  $\tilde{H}^{(0)}$  replaced by  $\tilde{H}$ ), and leads to the result:

$$\langle \delta\sigma \rangle_V = \left( \frac{e^2}{\pi\hbar} \right) \frac{1}{L^2} \sum_{\mathbf{Q}} \frac{1}{Q^2} = \left( \frac{e^2 D}{\pi\hbar} \right) \int_{\tau_{tr}}^{\tau_\phi} \frac{dt}{4\pi D t} \quad (1.71)$$

$$= \left( \frac{e^2 D}{\pi\hbar} \right) \int_{\tau_{tr}}^{\tau_\phi} P(0, t) dt \quad (1.72)$$

$$\simeq \frac{e^2}{\pi\hbar} \ln \frac{L_\phi}{l_e}. \quad (1.73)$$

The form of this correction appears reminiscent of its physical origin : it is due to the cooperon interference at a point before and after a diffusive travel around a loop. Thus this correction is proportional to the probability  $P(0, t)$  that this cooperon diffuses back to its origin on loops smaller than  $L_\phi$ ,

#### 1.4.2 Universal conductance fluctuations

We now consider the second cumulant  $\langle (\delta\sigma)^2 \rangle_V$  of the distribution function of conductivity, with  $\delta\sigma = \sigma - \langle \sigma \rangle_V$ . From the relation (1.37)  $\sigma = e^2 \rho(\epsilon_F) D$ , we expect the fluctuations of conductance  $\langle (\delta\sigma)^2 \rangle_V$  to originate either from fluctuations of the diffusion coefficient  $e^2 \rho(\epsilon_F) \langle \delta D \rangle_V$  or fluctuations of the density of states  $e^2 D \langle \delta \rho(\epsilon_F) \rangle_V$ . These two physical sources of fluctuations correspond to two different types of diagrams (Figs. 1.9 and 1.10). Their identification proceeds along the same lines as for the average conductivity : similarly than with a Lego game, we need to assemble the elementary blocks we have identified : the cooperon and diffuson structure factors and the Hikami boxes. The diffuson structure factor is deduced from that of the cooperon eq. (1.64) by time-reversal symmetry of the advanced branch: it reduces again to a projector on a single state, denoted the diffuson singlet defined in section 1.4.3:

$$\Gamma(\vec{q} = \vec{0}) = \frac{\gamma_V}{\tau_e} \frac{1}{Dq^2} \frac{1}{4} [\mathbf{I} \otimes \mathbf{I} + \sigma_x \otimes \sigma_x - \sigma_y \otimes \sigma_y + \sigma_z \otimes \sigma_z] \quad (1.74)$$

$$= \frac{\gamma_V}{\tau_e} \frac{1}{Dq^2} |\tilde{S}\rangle \langle \tilde{S}|. \quad (1.75)$$

Proceeding similarly than with cooperon, we identify a second renormalized Hikami box for diagrams involving diffuson structure factors in Fig. 1.9:

$$H = \rho(E_F) \left( \frac{2\tau_e}{\hbar} \right)^3 \frac{\pi}{16} [2 \mathbf{I} \otimes \mathbf{I} + \sigma^x \otimes \sigma^x + \sigma^y \otimes \sigma^y]. \quad (1.76)$$

The resulting contractions of the diagrams of figure 1.9 between two diffuson or cooperon structure factors lead to the result

$$\Delta\sigma_1^2 = 8 \left( \frac{e^2}{\hbar} \right)^2 \sum_{\vec{q}} \frac{1}{(L^2 q^2)^2}. \quad (1.77)$$

This contribution can be interpreted as describing the fluctuations of the diffusion coefficient  $D$  [4].

A second contribution to the conductance fluctuations originates from diagrams with a different topology, represented in Fig. 1.10. They describe the fluctuations of

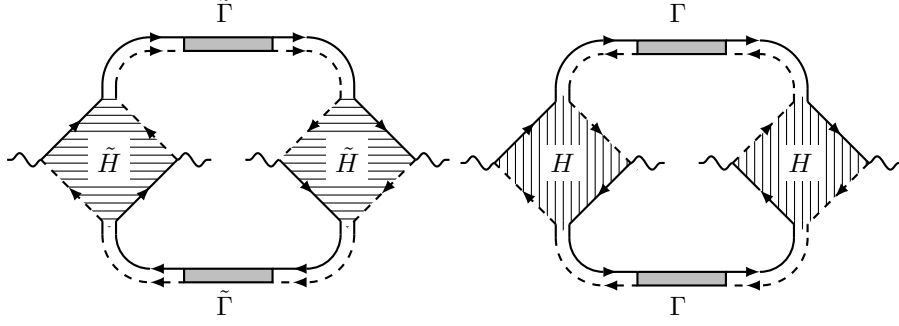


**Fig. 1.9** Diagrams describing the contributions to the conductivity fluctuations accounting for the fluctuations of the diffusion coefficient.

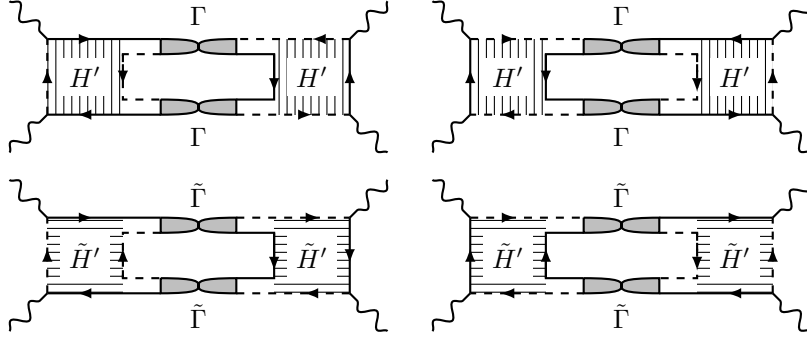


**Fig. 1.10** Diagrams describing the contributions to the conductivity fluctuations accounting for the fluctuations of the density of state.

the density of states  $\rho(\epsilon_F)$  [4]. Their determination requires two additional Hikami boxes:

$$H' = \rho(E_F) \left( \frac{2\tau_e}{\hbar} \right)^3 \frac{\pi}{16} [\mathbf{I} \otimes \mathbf{I} + \sigma^x \otimes \sigma^x] \quad (1.78)$$

$$\tilde{H}' = \rho(E_F) \left( \frac{2\tau_e}{\hbar} \right)^3 \frac{\pi}{16} [\mathbf{I} \otimes \mathbf{I} - \sigma^x \otimes \sigma^x]. \quad (1.79)$$

The final results after contraction in spin space of these diagrams is

$$\Delta\sigma_2^2 = 4 \left( \frac{e^2}{\hbar} \right)^2 \sum_{\bar{q}} \frac{1}{(L^2 q^2)^2}. \quad (1.80)$$

Summing the two contributions (1.77) and (1.80), we finally get the result:

$$\langle (\delta\sigma)^2 \rangle_V = 12 \left( \frac{e^2}{\hbar} \right)^2 \sum_{\bar{q}} \frac{1}{(L^2 q^2)^2} = \frac{12}{\pi^4} \left( \frac{e^2}{\hbar} \right)^2 \sum_{n_x \neq 0, n_y} \frac{1}{(n_x^2 + n_y^2)^2}. \quad (1.81)$$

The results (1.71,1.81) together define the quantum corrections to the diffusive transport of Dirac fermions in  $d = 2$ . They correspond exactly to known result of the Symplectic class in  $d = 2$ , and the previous calculations appear as a tedious way to recover these results for the specific case of Dirac fermions. In the next section, we will discuss that this is indeed the case by introducing the notion of universality class for quantum corrections to diffusive transport.

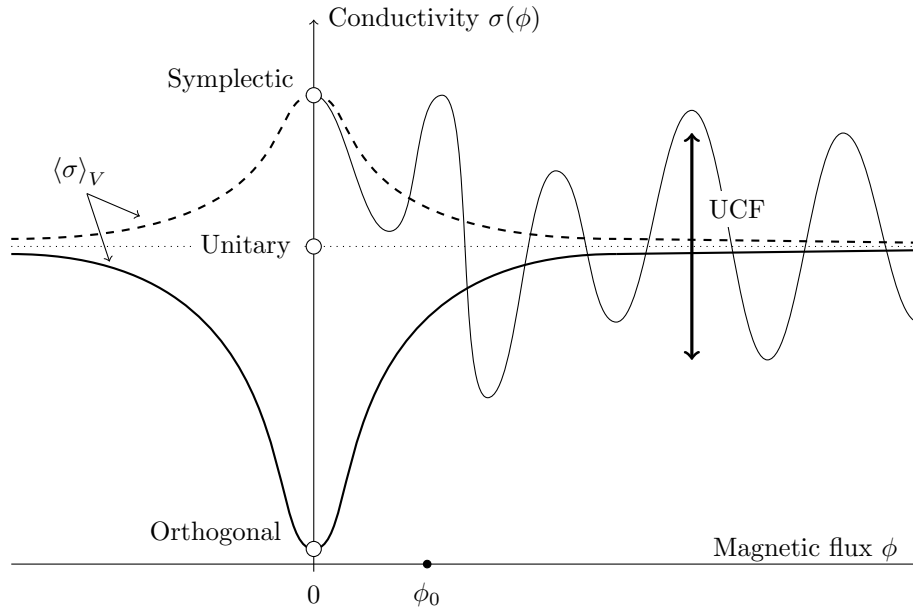


**Fig. 1.11** Schematic behavior of the quantum contribution to the averaged conductivity, observed in samples of size large compared with the phase coherent length scale  $L_\phi(T)$ , as a function of a weak magnetic field for different symmetry classes. (i) In the orthogonal class, corresponding *e.g.* to parabolic bands with charged impurities, a weak localization behavior is present which vanishes when a magnetic field is applied leading to the characteristic behavior represented by a plain line; (ii) In the symplectic class, corresponding *e.g.* to Dirac bands with charged impurities, the quantum correction at  $B = 0$  corresponds to a weak anti-localization, leading to the behavior represented by the dashed curve; (iii) When time reversal symmetry is broken (unitary class), no dependence on a weak magnetic field is observed (dotted line). For short samples of size comparable with  $L_\phi(T)$ , fluctuations of the conductivity occur as a functions of the magnetic field, characteristic of the unitary symmetry class.

### 1.4.3 Notion of universality class

*Universality class and number of diffusive modes.* In deriving diagrammatically the perturbation theory of weak localization, we have identified the building blocks as diffusive modes, either cooperon or diffuson, and the Hikami boxes that reconnect these

propagating modes to the current vertices. Moreover, we have found that the quantum corrections to the two first cumulants of the conductivity probability distribution function depends on the number of such Goldstone modes. This unusual universality strongly points towards an effective field theory approach underlying the above perturbation theory. This is indeed the case, and the non-linear sigma model developed to analyze the Anderson localization transitions turn out to be a very elegant framework to understand the universal results in the perturbative regime and classify all the possible universality classes [70], but also to derive in a systematic manner the higher cumulants of the conductivity probability distribution function [8]. In particular, the number of diffusive modes responsible for the quantum corrections to the conductance appear as the “dimension” of the target space of this effective field theory. This classification of symmetry classes of quantum transport has been recently used to analyze the occurrence of topological order in a gapped phase from the stability of their surface states with respect to disorder [50]. In this case, this stability manifests itself as a topological term allowed in the field theory action, which forbids Anderson localization. Such topological terms are irrelevant within the regime perturbative in disorder on which we focus here, and won't be discussed further.

A discussion of the field theory approach to the weak localization of electrons goes beyond the scope of the present lectures. A thorough discussion of the construction of the generating functional for the conductance moments can be found in ref. [8] (see also [22]) while a recent pedagogical introduction can be found in the textbook [7]. The general idea of this approach, inspired by the diagrammatic perturbative expansion presented in the previous section amounts to consider cumulants of pairs of Green's functions  $\mathcal{G}^R \mathcal{G}^A$  occurring in the Kubo formula (1.44). When doing so, the pairings between fermionic fields corresponding to both the cooperon and the diffuson modes are treated on equal footing. This amounts, after standard field theory techniques, to consider an action for the field

$$Q = \begin{pmatrix} d_{\uparrow\uparrow} & d_{\uparrow\downarrow} & -c_{\uparrow\downarrow} & c_{\uparrow\uparrow} \\ d_{\downarrow\uparrow} & d_{\downarrow\downarrow} & -c_{\downarrow\downarrow} & c_{\downarrow\uparrow} \\ c_{\downarrow\uparrow}^* & c_{\downarrow\downarrow}^* & d_{\downarrow\downarrow}^* & -d_{\downarrow\uparrow}^* \\ -c_{\uparrow\uparrow}^* & -c_{\uparrow\downarrow}^* & -d_{\uparrow\downarrow}^* & d_{\uparrow\uparrow}^* \end{pmatrix}, \quad (1.82)$$

where  $c, d$  corresponds to the modes in the cooperon and diffuson pairing channels (we consider spin  $\frac{1}{2}$  particles with no additional quantum number, as opposed to e.g. graphene). In a typical Landau approach, the dominant terms of this action in the long wavelength limit can be determined from symmetry constraints : the Goldstone modes of the resulting non-linear sigma model, corresponding to the diffusive cooperon and diffuson modes, are thus entirely determined by the dimension of space and the statistical symmetry of the disordered model. We summarize below the results of this approach.

The spin structure of the Dyson equation (1.51) reflects the construction of the diffuson as the tensor product of two spin  $\frac{1}{2}$  associated with the retarded and the advanced Green's function. It is thus naturally diagonalized by using the basis of singlet and triplet states for a spin  $\frac{1}{2}$  and a time reversed spin (with  $T|\uparrow\rangle = |\downarrow\rangle$  and  $T|\downarrow\rangle = -|\uparrow\rangle$ ):  $|S\rangle = \frac{1}{\sqrt{2}}(|\uparrow\uparrow\rangle + |\downarrow\downarrow\rangle)$ ,  $|T_1\rangle = \frac{1}{\sqrt{2}}(|\uparrow\uparrow\rangle - |\downarrow\downarrow\rangle)$ ,  $|T_2\rangle = |\uparrow\downarrow\rangle$ ,  $|T_3\rangle =$

$|\downarrow\uparrow\rangle$ . Similarly, the cooperon's structure factor is diagonalized in the basis of two spin  $\frac{1}{2}$ :  $|\tilde{S}\rangle = \frac{1}{\sqrt{2}}(|\uparrow\downarrow\rangle - |\downarrow\uparrow\rangle)$ ,  $|\tilde{T}_1\rangle = \frac{1}{\sqrt{2}}(|\uparrow\downarrow\rangle + |\downarrow\uparrow\rangle)$ ,  $|\tilde{T}_2\rangle = |\uparrow\uparrow\rangle$ ,  $|\tilde{T}_3\rangle = |\downarrow\downarrow\rangle$ . In these basis, the equation (1.51) and the equivalent one for the cooperon are diagonalized for each state : the various diffuson and cooperon modes propagate either diffusively or not. We can write formally

$$\Gamma_{S/T}(\vec{q}) = \frac{\gamma_V}{\tau_e} \frac{1}{Dq^2 + \eta_\phi + \eta^{D,S/T}}, \quad ; \quad \tilde{\Gamma}_{S/T}(\vec{Q}) = \frac{\gamma_V}{\tau_e} \frac{1}{DQ^2 + \eta_\phi + \eta^{C,S/T}}, \quad (1.83)$$

with  $\eta_\phi = \hbar/\tau_\phi$ . The various dephasing rates account for the possible decay over short length scale of the respective mode :  $\eta^{C/D,S/T} = 0$  for diffusive mode while it is finite for modes contributing only on short length scales (cross-over between different universality classes can be described along these lines [23]).

The general expression for the quantum correction to the averaged conductivity is the sum of contributions

$$\langle \delta\sigma \rangle_V = -\frac{e^2 D}{\pi \hbar} \left[ -\frac{1}{4} \frac{1}{L^d} \sum_{\mathbf{Q}} \frac{1}{DQ^2 + \eta_S^{(C)} + \eta_\phi} + \frac{1}{4} \sum_{\alpha} \frac{1}{L^d} \sum_{\mathbf{Q}} \frac{1}{DQ^2 + \eta_{T_\alpha}^{(C)} + \eta_\phi} \right], \quad (1.84)$$

where  $d$  is the dimensionality of diffusion. In this expression, the cooperon singlet mode occurs as a negative correction, while all triplet modes contribute a positive correction : this quantum correction thus depends solely on the number of modes of the cooperon structure factor. The different symmetry classes, initially identified through random matrix considerations (see [15] for a general review), correspond to different number of cooperon modes :

- in situation with spin rotation symmetry, corresponding to a spinless Hamiltonian with a time-reversal situation  $T^2 = \mathbf{I}$ , all cooperon modes are present and contribute to the quantum correction, which is negative. This corresponds to the weak-localization situation.
- when spin-momentum locking occurs, either due to the pure Hamiltonian (Dirac case) or due to the disorder type (spin-orbit disorder), all triplet modes are affected and cannot diffuse on long distances. Only the singlet modes contribute to (1.84) and we find a weak anti-localization. This corresponds to a situation where time-reversal symmetry satisfies  $T^2 = -\mathbf{I}$ . Note that the  $d = 2$  situation of random spin-orbit is special as disorder only affects the  $z$  components of spins : one triplet and one singlet modes remains unaffected and we obtain a "pseudo-unitary" class [31]
- finally when spin symmetry is broken, either by magnetic impurities or a magnetic field, no cooperon modes diffuse and we obtain a vanishing quantum correction.

These three cases are summarized on the table 1.1.

Similarly the amplitude of conductance fluctuations can be written as the sum of contribution from the different diffusive modes

	scalar disorder	random spin-orbit	magnetic disorder
quadratic dispersion	Orthogonal	Symplectic (d=3) Pseudo Unitary (d=2)	Unitary
Dirac dispersion	Symplectic	Symplectic	Unitary

**Table 1.1** Summary of the symmetry classes for the different types to disorder for quadratic and Dirac Hamiltonians.

Symmetry Class	TRS symmetry	diffuson modes	cooperon modes	weak localization	UCF
Orthogonal	$T^2 = \mathbf{I}$	1 S + 3 T	1S + 3T	-2	8
Symplectic	$T^2 = -\mathbf{I}$	1 S	1S	+1	2
Unitary	0	1 S	0	0	1

**Table 1.2** Summary of the number of singlet (S) and triplet (T) modes for the cooperon and diffuson structure factors. The weak localization contributions are represented as respective integer factors depending solely on the numbers of diffusive modes. The corresponding proportionality factors are defined in eqs.(1.84,1.85)

$$\begin{aligned} \langle (\delta\sigma)^2 \rangle_V = & F(\eta_m^{D,S} + \eta_\phi) + \sum_{\alpha=1,2,3} F(\eta_m^{D,T_\alpha} + \eta_\phi) \\ & + F(\eta_m^{C,S} + \eta_\phi) + \sum_{\alpha=1,2,3} F(\eta_m^{C,T_\alpha} + \eta_\phi) \end{aligned} \quad (1.85)$$

where

$$F(\eta) = 6 \sum_{\bar{q}} \frac{1}{((Lq)^2 + \eta)^2}. \quad (1.86)$$

Hence the conductance fluctuations depends linearly on the number of diffusive modes. This is summarized in table 1.2.

#### 1.4.4 Effect of a magnetic field

*Transverse magnetic field.* In the presence of a magnetic field, the probability of return to the origin during time  $t$  of a diffusive walk is modified into [4] :

$$Z_c(t, B) = \frac{\phi/\phi_0}{\sinh(4\pi B D t / \phi_0)} \quad (1.87)$$

where  $\phi = BL^2$  and the argument of the sinh function is the dimensionless magnetic flux through the region  $4\pi l_t^2$  typically explored by the diffusive path during time  $t$  :  $l_t^2 = Dt$ . The corresponding quantum contribution to the conductivity can be written as

$$\langle \delta\sigma(B) \rangle_V = (\# C, S - \# C, T) \frac{e^2 D}{\pi \hbar} \int_{\tau_{tr}}^{\tau_\phi} Z_c(t, B) \quad (1.88)$$

$$= (\# C, S - \# C, T) \left[ \Psi \left( \frac{1}{2} + \frac{\hbar}{4eDB\tau_{tr}} \right) - \Psi \left( \frac{1}{2} + \frac{\hbar}{4eDB\tau_\phi} \right) \right] \quad (1.89)$$

where  $\Psi(x)$  is a digamma function. This formula is commonly used as a fit to extract the phase coherent time  $\tau_\phi$  from experimental transport measurements. Note that in this case, the expression (1.89) describes a cross-over from the orthogonal or symplectic class at  $B = 0$  to the unitary class at larger magnetic field.

*Aharonov-Bohm like oscillations.* Finally we consider a cylinder made out of a topological insulating material, with a metallic Dirac metal at its surface (see Fig. 1.12). The cylinder is considered long compared to the dephasing length scale  $L_\phi(T)$  so that conductance fluctuations are negligible (they are statistically reduced by the incoherent combination of contributions of domains of size  $L_\phi(T)$ ). This conductivity is thus well described by its average  $\langle\sigma\rangle_V$ , which consist of both the classical contribution and the quantum correction. This quantum correction is due to the contribution of cooperon diffusive modes. When a magnetic flux is threaded through the section of the cylinder, this cooperon which carries a charge  $2e$  acquires an Aharonov-Bohm phase, leading to oscillations of the quantum contribution to the conductivity with a period  $\tilde{\phi}_0 = h/(2e)$ . As depicted on Fig.1.12, the phase of these oscillations is fixed by the

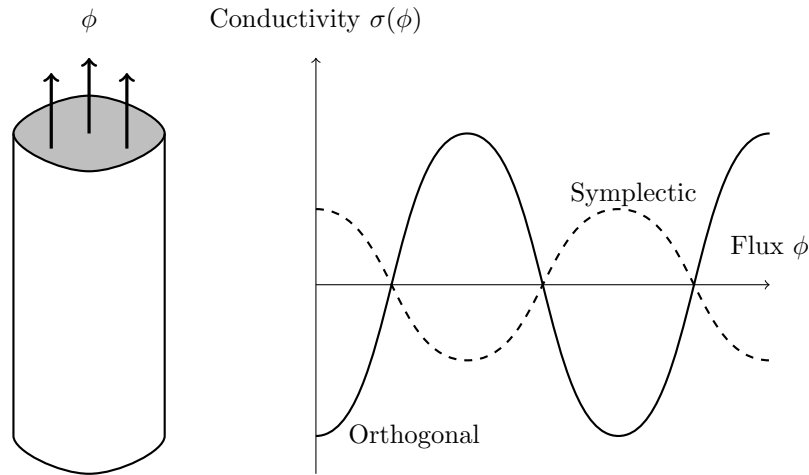


**Fig. 1.12** Schematic representation of the Aharonov-Bohm oscillations of a metal at the surface of a cylinder. In the case of Dirac particles, we expect a behavior predicted by the Symplectic symmetry class.

sign of the quantum correction at  $\phi = 0$ , and thus the symmetry class. In the case of Dirac fermions, these oscillations are reminiscent of the  $\pi$  phase acquired due to momentum-spin locking by particles when winding around the cylinder in the ballistic limit. However the absolute phase of these ballistic oscillations is very sensitive to energy which renders it hard to measure experimentally. See [11, 68] for a recent discussion of this effect in the context of topological insulators' surface states, and [12] for a detailed discussion. This concludes our introductory lectures to the transport properties of Dirac surface states.

*Acknowledgment* : I warmly thank P. Adroguer, J. Cayssol, A. Fedorenko, G. Montambaux and E. Orignac with whom I learned most of what is included in these lectures. I am particularly indebted to P. Adroguer for a recent stimulating discussion on the pseudo-unitary class in two dimensions and E. Orignac for proof reading this manuscript.

# References

- [1] Adam, S., Brouwer, P.W., and Sarma, S. Das (2009). Crossover from quantum to Boltzmann transport in graphene. *Phys. Rev. B*, **79**, 201404 (R).
- [2] Adam, S., Hwang, E. H., Galitski, V. M., and Sarma, S. Das (2007). A self-consistent theory for graphene transport. *Proc. Natl. Acad. Sci. U.S.A.*, **104**, 18392.
- [3] Adroguer, P., Carpentier, D., Cayssol, J., and Orignac, E. (2012). Diffusion at the surface of topological insulators. *New Journal of Physics*, **14**, 103027.
- [4] Akkermans, E. and Montambaux, G. (2007). *Mesoscopic Physics of electrons and photons*. Cambridge University Press.
- [5] Aleiner, I. L. and Efetov, K. B. (2006). Effect of disorder on transport in graphene. *Phys. Rev. Lett.*, **97**, 236801.
- [6] Altland, Alexander (2006). Low-energy theory of disordered graphene. *Phys. Rev. Lett.*, **97**, 236802.
- [7] Altland, A. and Simons, Ben (2010). *Condensed Matter Field Theory*. Cambridge University Press.
- [8] Altshuler, B.L., Kravtsov, V.E., and Lerner, I.V. (1991). Distribution of mesoscopic fluctuations and relaxation properties in disordered conductors. In *Mesoscopic Phenomena in Solids* (ed. B. L. Altshuler, P. A. Lee, and R. A. Webb), p. 449. North-Holland, Amsterdam.
- [9] Altshuler, B. L., Lee, P. A., and Webb, R. A. (ed.) (1991). *Mesoscopic Phenomena in Solids*. North-Holland, Amsterdam.
- [10] Ando, Tsuneya (2008). Physics of graphene. *Prog. Theor. Phys. Suppl.*, **176**, 203.
- [11] Bardarson, J. H., Brouwer, P.W., and Moore, J. E. (2010). Aharonov-Bohm oscillations in disordered topological insulator nanowires. *Phys. Rev. Lett*, **105**, 156803.
- [12] Bardarson, J. H. and Moore, J.E. (2013). Quantum interference and aharonov-bohm oscillations in topological insulators. *Rep. Prog. Phys.*, **76**, 056501.
- [13] Bardarson, J. H., Tworzydło, J., Brouwer, P. W., and Beenakker, C. W. J. (2007). One-parameter scaling at the Dirac point in graphene. *Phys. Rev. Lett.*, **99**, 106801.
- [14] Beenakker, C.W.J. (2008). Colloquium: Andreev reflection and Klein tunneling in graphene. *Rev. Mod. Phys.*, **80**, 1337.
- [15] Beenakker, C. W. J. (1997). Random-matrix theory of quantum transport. *Rev. Mod. Phys.*, **69**, 731.
- [16] Bena, C. and Montambaux, G. (2009). Remarks on the tight-binding model of graphene. *New J. Phys.*, **11**, 095003.
- [17] Berry, M. V. (1984). Quantal phase factors accompanying adiabatic changes. *Proceedings of the Royal Society of London. A. Mathematical and Physical Sci-*

- ences, **392**, 45–57.
- [18] Bouchiat, H., Guéron, S., Montambaux, G., and Dalibard, J. (ed.) (2004). *Nanophysics : Coherence and Transport, Les Houches School, Session LXXXI*. Elsevier.
  - [19] Castro Neto, A. H., Guinea, F., Peres, N. M. R., Novoselov, K. S., and Geim, A. K. (2009). The electronic properties of graphene. *Rev. Mod. Phys.*, **81**, 109.
  - [20] Das Sarma, S., Adam, S., Hwang, E. H., and Rossi, E. (2011). Electronic transport in two-dimensional graphene. *Rev. Mod. Phys.*, **83**, 407.
  - [21] Dyson, F. J. (1962). The threefold way. Algebraic structure of symmetry groups and ensembles in quantum mechanics. *J. Math. Phys.*, **3**, 1199.
  - [22] Efetov, K.B., Larkin, A.I., and Khmel'nitskii, D.E. (1980). Interaction of diffusion modes in the theory of localization. *Sov. Phys. JETP*, **52**, 568–574.
  - [23] Fedorenko, A. A. and Carpentier, D. (2009). Magnetic dephasing in a mesoscopic spin glass. *Europhys. Lett.*, **88**, 57009.
  - [24] Foa Torres, L.E.F., Roche, S., and Charlier, J.-C. (2014). *Introduction to Graphene-based Nanomaterials*. Cambridge University Press.
  - [25] Fradkin, Eduardo (1986). Critical behavior of disordered degenerate semiconductors. I. Models, symmetries, and formalism. *Phys. Rev. B*, **33**, 3257.
  - [26] Fradkin, Eduardo (1986). Critical behavior of disordered degenerate semiconductors. II. Spectrum and transport properties in mean-field theory. *Phys. Rev. B*, **33**, 3263.
  - [27] Fruchart, M., Carpentier, D., and Gawedzki, K. (2014). Parallel transport and band theory in crystals. *Europhys. Lett.*, **106**, 60002.
  - [28] Fu, L. (2009). Hexagonal warping effects in the surface states of the topological insulator  $\text{Bi}_2\text{Te}_3$ . *Phys. Rev. Lett.*, **103**, 266801.
  - [29] Hasan, M. Z. and Kane, C. L. (2010). Colloquium: Topological insulators. *Rev. Mod. Phys.*, **82**, 3045–3067.
  - [30] Hatsugai, Y., Morimoto, T., Kawarabayashi, T., Hamamoto, Y., and Aoki, H. (2013). Chiral symmetry and its manifestation in optical responses in graphene: interaction and multilayers. *New Journal of Physics*, **15**, 035023.
  - [31] Hikami, S., Larkin, A., and Nagaoka, Y. (1980). Spin-orbit interaction and magnetoresistance in the two dimensional random system. *Prog. Theor. Phys.*, **63**, 707.
  - [32] Imry, Y. (2002). *Introduction to mesoscopic physics*. Oxford University Press.
  - [33] Itzykson, C. and Drouffe, J.-M. (1991). *Statistical Field Theory: Volume 1*. Cambridge University Press.
  - [34] Katsnelson, M. I. (2006). Zitterbewegung, chirality, and minimal conductivity in graphene. *Eur. Phys. J. B*, **51**, 157.
  - [35] Katsnelson, M. I. (2012). *Graphene: Carbon in Two Dimensions*. Cambridge University Press.
  - [36] Khveshchenko, D. V. (2006). Electron localization properties in graphene. *Phys. Rev. Lett.*, **97**, 036802.
  - [37] Langer, J.L. and Neal, T. (1966). Breakdown of the concentration expansion for the impurity resistivity of metals. *Phys. Rev. Lett.*, **16**, 984.
  - [38] Li, Q., Rossi, E., and Sarma, S. Das (2012). Two-dimensional electronic transport

- on the surface of three-dimensional topological insulators. *Phys. Rev. B*, **86**, 235443.
- [39] Liu, C.-X., Qi, X.-L., Zhang, H., Dai, X., Fang, Z., and Zhang, S.-C. (2010). Model hamiltonian for topological insulators. *Phys. Rev. B*, **82**, 045122.
- [40] Ludwig, A. W. W., Fisher, M. P. A., Shankar, R., and Grinstein, G. (1994). Integer quantum hall transition: An alternative approach and exact results. *Phys. Rev. B*, **50**, 7526.
- [41] Marder, Michael P. (2010). *Condensed Matter Physics*. Wiley-Blackwell.
- [42] McCann, E., Kechedzhi, K., Fal'ko, V.I., Suzuura, H., Ando, T., and Altshuler, B.L. (2006). Weak-localization magnetoresistance and valley symmetry in graphene. *Phys. Rev. Lett.*, **97**, 146805.
- [43] Morpurgo, A. F. and Guinea, F. (2006). Intervalley scattering, long-range disorder, and effective time-reversal symmetry breaking in graphene. *Phys. Rev. Lett.*, **97**, 196804.
- [44] Nielsen, H. B. and Ninomiya, M. (1981). No go theorem for regularizing chiral fermions. *Phys. Lett.*, **105**, 219.
- [45] Nomura, K., Koshino, M., and Ryu, S. (2007). Topological delocalization of two-dimensional massless dirac fermions. *Phys. Rev. Lett.*, **99**, 146806.
- [46] Peres, N. M. R., Guinea, F., and Castro Neto, A. H. (2006). Electronic properties of disordered two-dimensional carbon. *Phys. Rev. Lett.*, **73**, 125411.
- [47] Qi, X.-L. and Zhang, S.-C. (2011). Topological insulators and superconductors. *Rev. Mod. Phys.*, **83**, 1057.
- [48] Ringel, Z., Kraus, Y., and Stern, A. (2012). Strong side of weak topological insulators. *Phys. Rev. B*, **86**, 045102.
- [49] Ryu, S., Mudry, C., Furusaki, A., and Ludwig, A. W. W. (2007). Landauer conductance and twisted boundary conditions for dirac fermions in two space dimensions. *Phys. Rev. B*, **75**, 205344.
- [50] Ryu, S., Schnyder, A. P., Furusaki, A., and Ludwig, A. W. W. (2010). Topological insulators and superconductors: tenfold way and dimensional hierarchy. *New Journal of Physics*, **12**, 065010.
- [51] San-Jose, P., Prada, E., and Golubev, D.S. (2007). Universal scaling of current fluctuations in disordered graphene. *Phys. Rev. B*, **76**, 195445.
- [52] Schneider, M. and Brouwer, P.W. (2014). Quantum corrections to transport in graphene: a trajectory-based semiclassical analysis. *New Journal of Physics*, **16**, 073015.
- [53] Schuessler, A., Ostrovsky, P. M., Gornyi, I. V., and Mirlin, A. D. (2009). Analytic theory of ballistic transport in disordered graphene. *Phys. Rev. B*, **79**, 075405.
- [54] Shon, N. H. and Ando, T. (1998). Quantum transport in two-dimensional graphite system. *J. Phys. Soc. Jpn.*, **67**, 2421.
- [55] Sondheimer, E.H. (1962). The Boltzmann equation for anisotropic metals. *Proc. R. Soc. London, Ser. A*, **268**, 100.
- [56] Sorbello, R.S. (1974). On the anisotropic relaxation time. *J. Phys. F*, **4**, 503.
- [57] Sorbello, R.S. (1975). Effects of anisotropic scattering on electronic transport properties. *Phys. Cond. Matter*, **19**, 303.
- [58] Sundaram, G. and Niu, Q. (1999). Wave-packet dynamics in slowly perturbed

- crystals: Gradient corrections and Berry-phase effects. *Phys. Rev. B*, **59**, 14915.
- [59] Suzuura, H. and Ando, T. (2002). Crossover from symplectic to orthogonal class in a two-dimensional honeycomb lattice. *Phys. Rev. Lett.*, **89**(26), 2666603.
- [60] Tkachov, G. and Hankiewicz, E. M. (2011). Weak antilocalization in HgTe quantum wells and topological surface states: Massive versus massless Dirac fermions. *Phys. Rev. B*, **84**, 035444.
- [61] Tsypliyatyev, O., Aleiner, I.L., Fal'ko, V.I., and Lerner, I.V. (2009). Applicability of the ergodic hypothesis to mesoscopic fluctuations. *Phys. Rev. B*, **68**, 121301.
- [62] Tworzydło, J., Trauzettel, B., Titov, M., Rycerz, A., and Beenakker, C. W. J. (2006). Sub-poissonian shot noise in graphene. *Phys. Rev. Lett.*, **96**, 246802.
- [63] Vafeek, O. and Vishwanath, A. (2014). Dirac fermions in solids - from high Tc cuprates and Graphene to topological insulators and Weyl semimetals. *Annual Review of Condensed Matter Physics*, **5**, 83.
- [64] W. Zawadzki, T. M. Rusin (2011). Zitterbewegung (trembling motion) of electrons in semiconductors: a review. *J. Phys. Condens. Matter*, **23**, 143201.
- [65] Wakabayashi, K., Takane, Y., Yamamoto, M., and Sigrist, M. (2009). Electronic transport properties of graphene nanoribbons. *New J. Phys.*, **11**, 095016.
- [66] Wigner, E.P. (1959). *Group Theory and its Application to the Quantum Mechanics of Atomic Spectra*. Academic Press.
- [67] Xiao, D., Chang, M.-C., and Niu, Q. (2010). Berry phase effects on electronic properties. *Rev. Mod. Phys.*, **82**, 1959–2007.
- [68] Zhang, Y. and Vishwanath, A. (2010). Anomalous Aharonov-Bohm conductance oscillations from topological insulator surface states. *Phys. Rev. Lett.*, **105**, 206601.
- [69] Ziegler, K. (1998). Delocalization of 2D Dirac fermions: The role of a broken supersymmetry. *Phys. Rev. Lett.*, **80**, 3113.
- [70] Zirnbauer, M.R. (1996). Riemannian symmetric superspaces and their origin in random-matrix theory. *J. Math. Phys.*, **37**, 4986.
- [71] Zirnbauer, Martin (2011). *The Oxford Handbook of Random Matrix Theory*, Chapter 3 : Symmetry Classes. Oxford University Press.